UNIVERSIDAD DE CONCEPCIÓN

Centro de Investigación en Ingeniería Matemática (CI^{2}MA)

Antidiffusive Lagrangian-remap schemes for models of polydisperse sedimentation

Raimund Bürger, Christophe Chalons,
Luis M. Villada

PREPRINT 2015-04

SERIE DE PRE-PUBLICACIONES

ANTIDIFFUSIVE LAGRANGIAN-REMAP SCHEMES FOR MODELS OF POLYDISPERSE SEDIMENTATION

RAIMUND BÜRGER[A], CHRISTOPHE CHALONS[B], AND LUIS M. VILLADA[C]

Abstract. Models of sedimentation of polydisperse suspensions of small particles in a viscous fluid that belong to N size classes give rise to systems of N strongly coupled, nonlinear first-order conservation laws for the local solids volume fractions as functions of depth and time. The settling velocities usually have variable sign depending on local fluctuations of the density of the mixture, and the model is posed with zero-flux boundary conditions for batch settling in a column. Since the eigenvalues and eigenvectors of the flux Jacobian have no closed algebraic form, characteristic-wise numerical schemes for these models become involved. Alternative simple schemes for this model directly utilize the velocity functions and are based on splitting the system of conservation laws into two different first-order quasi-linear systems, which are solved successively for each time iteration, namely, the Lagrangian and remap steps (so-called Lagrangian-remap (LR) schemes). This approach was advanced in [R. Bürger, C. Chalons and L.M. Villada, SIAM J. Sci. Comput. 35 (2013) B1341–B1368] for a multiclass Lighthill-Whitham-Richards traffic model with nonnegative velocities. By incorporating recent antidiffusive techniques for transport equations a new version of these Lagrangian-antidiffusive remap (L-AR) schemes for the polydisperse sedimentation model is constructed. These L-AR schemes are supported by a partial analysis for $N = 1$. They are total variation diminishing under a suitable CFL condition and therefore converge to a weak solution. Numerical examples for several values of N illustrate that these schemes, including a more accurate version based on MUSCL extrapolation, are competitive in accuracy and efficiency with several existing schemes.

1. Introduction

1.1. **Scope.** Models of sedimentation of polydisperse suspensions of small spherical particles suspended in a viscous fluid can be posed as systems of strongly coupled nonlinear first-order conservation laws

$$\partial_t \Phi + \partial_x \boldsymbol{f}(\Phi) = \mathbf{0}, \quad x \in (0, L), \quad t > 0, \tag{1.1}$$

where x denotes vertical distance, t is time, $\phi_i = \phi_i(x, t)$ is the local volume fraction of particles of species i having diameter d_i and density ϱ_i, where we assume $d_1 \geq d_2 \geq \cdots \geq d_N$. Moreover, $\Phi = (\phi_1, \ldots, \phi_N)^{\mathrm{T}}$ and $\boldsymbol{f}(\Phi) = (f_1(\Phi), \ldots, f_N(\Phi))^{\mathrm{T}}$, where

$$f_i(\Phi) = \phi_i v_i(\Phi), \quad i = 1, \ldots, N, \tag{1.2}$$

and $v_i(\Phi)$ is the velocity of particle species i, which is assumed to be a given function of Φ. Several algebraic forms of the velocity functions $v_i(\Phi)$ have been proposed in the literature. We here focus on choices for which these velocity functions have variable sign and at the same time the system (1.1) is strictly hyperbolic, i.e., the eigenvalues of the Jacobian matrix $\mathcal{J}_{\boldsymbol{f}}(\Phi) = (\partial f_i(\Phi)/\partial \phi_j)_{1 \leq i,j \leq N}$ are real and pairwise distinct (under determined circumstances). Batch sedimentation of a suspension of given initial composition in a column of height L is then modeled by (1.1) under the specific assumption (1.2) along with the initial condition

$$\Phi(x, 0) = \Phi_0(x), \quad x \in (0, L) \tag{1.3}$$

Date: January 16, 2015.

Key words and phrases. System of conservation laws, Lagrangian-remap scheme, antidiffusive scheme, sedimentation, polydisperse suspension.

[A]CI^{2}MA and Departamento de Ingeniería Matemática, Facultad de Ciencias Físicas y Matemáticas, Universidad de Concepción, Casilla 160-C, Concepción, Chile. E-Mail: rburger@ing-mat.udec.cl.

[B]Laboratoire de Mathématiques de Versailles, UMR 8100, Université de Versailles Saint-Quentin-en-Yvelines, UFR des Sciences, bâtiment Fermat, 45 avenue des Etats-Unis, 78035 Versailles cedex, France. E-mail: christophe.chalons@uvsq.fr.

[C]Departamento de Matemática, Universidad del Bío-Bío, Casilla 5-C, Concepción, Chile. E-Mail: lvillada@ubiobio.cl.

and zero-flux boundary conditions

$$f_i|_{x=0} = f_i|_{x=L} = 0, \quad i = 1, \ldots, N, \tag{1.4}$$

where we assume that $\Phi_0 \in (L^1(0,L))^N$, and that Φ_0 takes values in the set $\mathcal{D}_{\phi_{\max}}$ of physically relevant concentration vectors defined by

$$\mathcal{D}_{\phi_{\max}} := \big\{(\phi_1, \ldots, \phi_N)^{\mathrm{T}} \in \mathbb{R}^N : \phi_1 \geq 0, \ldots, \phi_N \geq 0,\, \phi_1 + \cdots + \phi_N \leq \phi_{\max}\big\}, \tag{1.5}$$

where $\phi_{\max}$ is a maximum total solids concentration.

It is well known that even if Φ_0 is smooth, solutions of (1.1), (1.3) develop discontinuities, and so we seek a weak solution. If a weak solution Φ has a discontinuity along a smooth curve $x = x(t)$ and Φ is continuous on either side of $x(t)$ with limits Φ_- and Φ_+ to the left and right of the jump, respectively, then the Rankine-Hugoniot jump condition $\boldsymbol{f}(\Phi_+) - \boldsymbol{f}(\Phi_-) = s(\Phi_+ - \Phi_-)$ must be satisfied, where $s = \mathrm{d}x/\mathrm{d}t$ is the shock speed.

The numerical solution of (1.1)–(1.4) is a challenge since the eigenvalues and eigenvectors of $\mathcal{J}_{\boldsymbol{f}}(\Phi)$ are not available in closed form, so numerical schemes that rely on characteristic information become fairly involved (but are still competitive in efficiency [10, 17]). Alternatively, one can construct easy-to-implement numerical schemes for (1.1), (1.2) by exploiting the concentration-times-velocity form (1.2) of the fluxes. These properties were first used in [12] to design simple difference schemes for (1.1)–(1.4).

It is the purpose of this paper to advance a new class of schemes for (1.1)–(1.4) that do not rely on spectral (characteristic) information and are as easy to implement as the schemes introduced in [12], but are more accurate and efficient. This work extends the Lagrangian–antidiffusive remap (L-AR) methods introduced in [8] to the model of polydisperse sedimentation. In [8] L-AR methods are applied to the multiclass Lighthill-Whitham-Richards (MCLWR) model for vehicular traffic [5, 34]. The main new difficulties that arise with the present model of polydisperse sedimentation are the more involved algebraic form of the functions $v_i(\Phi)$, which may have variable sign while those of the MCLWR model are nonnegative, and the presence of the boundary conditions (1.4).

To explain the main idea of L-AR schemes, consider the scalar continuity equation for a single species:

$$\partial_t \phi + \partial_x\big(\phi v(\phi)\big) = 0, \quad x \in (0,L), \quad t > 0. \tag{1.6}$$

We formally rewrite (1.6) as

$$\partial_t \phi + \phi \partial_x\big(v(\phi)\big) + v(\phi)\partial_x \phi = 0, \quad x \in (0,L), \quad t > 0. \tag{1.7}$$

The new class of schemes for (1.6) is based on splitting (1.7) into two different equations, which are solved alternatingly. To advance the solution from time t to $t + \Delta t$, we first apply a Lagrangian method [19] to solve

$$\partial_t \phi + \phi \partial_x v(\phi) = 0, \tag{1.8}$$

and use this solution, evolved over a time interval of length Δt, as the initial condition for solving in a second step the transport equation

$$\partial_t \phi + v(\phi)\partial_x \phi = 0, \tag{1.9}$$

whose solution, again evolved over a time interval of length Δt, provides the sought approximate solution of (1.6) valid for $t + \Delta t$. These steps will be identified as "Lagrangian" and "remap" steps, respectively, which explains why the schemes under study are addressed as "Lagrangian-remap" (LR) schemes. The specific idea behind "Lagrangian-antidiffusive remap" L-AR schemes is to solve (1.9) by recent antidiffusive techniques for transport equations, and thereby to increase the overall efficiency of the proposed splitting strategy, while keeping its simplicity. In fact, one can employ an antidiffusive but stable numerical scheme [6, 7, 16] for (1.9), where the scheme for this remap step is designed in such a way that the resulting scheme (first step followed by second step) is conservative. In [8] we discuss several variants of L-AR schemes defined by different choices of th numerical flux. Based in part on experience gained in that paper we herein focus on the so-called NBee method [6], which has been found suitable for velocities with variable sign.

Alternatively, the remap step can be handled by a random sampling technique, giving rise to a Lagrangian-random sampling (L-RS) subclass of LR schemes. While both L-AR and L-RS schemes can readily be extended to the multiple-species case ($N > 1$), performance of L-AR schemes has turned out superior to

that of L-RS schemes for the polydisperse sedimentation model. Moreover, the description of L-RS schemes for the present problem is identical to that for the MCLWR model in [8], so these schemes are not discussed herein.

The use of LR schemes for the polydisperse sedimentation model is supported by a partial analysis of the L-AR schemes for $N = 1$, with the conclusion that under suitable CFL conditions, these schemes have the total variation diminishing (TVD) property and therefore converge to a weak solution. Numerical experiments show that the proposed schemes are competitive with those introduced in [12].

1.2. **Related work.** Models of polydisperse sedimentation with velocities of variable sign and proven hyperbolicity property include the Masliyah-Lockett-Bassoon (MLB) model [24, 26], the modified MLB (MMLB) model due to Basson et al. [2], and the Davis-Gecol (DG) model [15], whose respective precise algebraic form will be stated in Section 2.1. Other models such as the one by Höfler and Schwarzer [20] give rise to functions $v_i(\Phi)$ of constant sign, are therefore very similar to the MCLWR model for vehicular traffic [5, 34] studied in [8], and will not be chosen for detailed study herein.

Antidiffusive numerical schemes have been advanced in the pioneering work by Després and Lagoutière [16] for the linear transport equation with application to gas dynamics, and then extended to monotone scalar conservation laws by Bouchut [7] and applied to Hamilton-Jacobi-Bellman equations by Bokanowski and Zidani in [6]. We refer to [21, 23] and the references therein for further extensions.

1.3. **Outline of the paper.** The remainder of this paper is organized as follows. Section 2 collects some preliminaries. In particular, in Section 2.1 we introduce the models of polydisperse sedimentation that motivate the new version of L-AR schemes and are chosen for numerical experiments. In Section 2.2 we summarize two simple difference schemes from [12], namely a first-order scheme and its second-order version. These schemes are selected as a reference to assess the performance of the new version of L-AR schemes. Section 3 is devoted to the presentation, and partial analysis, of the new L-AR schemes. To this end we introduce in Section 3.1 the spatial discretization. The following discussion of discretizations of the scalar equation (1.6) is based in three different cases. We first assume that $v(\phi) \leq 0$ and $v'(\phi) \geq 0$ for $0 \leq \phi \leq \phi_{\max}$ (Case 1), and outline in Sections 3.2, 3.3 and 3.4 the discretization of the Lagrangian step, the discretization of the remap step, and the complete L-AR scheme for this case, respectively. Section 3.3 includes, in particular, a description of the NBee scheme proposed by Bokanowski and Zidani in [6] that forms the antidiffusive scheme for the discretization of the remap step. Corresponding results for (1.6) under the assumptions $v(\phi) \geq 0$ and $v'(\phi) \leq 0$ for $0 \leq \phi \leq \phi_{\max}$ (Case 2) were obtained in [8] and are summarized in Section 3.5. Based on the treatment of Sections 3.2 to 3.5, we define in Section 3.6 L-AR schemes for Case 3 of (1.6), namely when both $v(\phi)$ and $v'(\phi)$ may have variable sign. These schemes motivate the presentation of L-AR schemes for $N \geq 1$ provided in Section 3.7. Finally, we present in Section 3.8 a version of the L-AR schemes for general N whose spatial accuracy is improved by MUSCL extrapolation. Numerical examples are presented in Section 4, and conclusions are collected in Section 5.

2. Preliminaries

2.1. **Models of polydisperse sedimentation.** We assume that $v_1, \dots, v_N$ are smooth functions of Φ on $\mathcal{D}_{\phi_{\max}}$, and that $v_i(\Phi) = 0$ wherever $\phi \geq \phi_{\max}$. For the formulation of CFL conditions and the hyperbolicity analysis we assume furthermore that $v_1, \dots, v_N$ do not depend on each of the N components of Φ, but on a number $m \ll N$ of scalar functions of Φ. Thus, with a slight abuse of notation, we have

$$v_i = v_i\big(p_1(\Phi), \dots, p_m(\Phi)\big), \quad i = 1, \dots, N, \tag{2.1}$$

where we assume that $v_1, \dots, v_N$ are Lipschitz continuous functions with respect to each argument $p_1, \dots, p_m$. In this case, $\mathcal{J}_{\boldsymbol{f}}(\Phi)$ becomes a rank-m perturbation of a diagonal matrix. This property has made it possible to estimate the hyperbolicity region for a number of polydisperse sedimentation models with $m \leq 4$ (see [9, 11]) by the so-called secular equation [1, 18]. The hyperbolicity and the interlacing of the (unknown) eigenvalues of $\mathcal{J}_{\boldsymbol{f}}(\Phi)$ with the (known) velocities $v_1, \dots, v_N$ form the key ingredients for the construction of efficient characteristic-wise (spectral) weighted essentially non-oscillatory (WENO) schemes for (1.1), denoted "WENO-SPEC-INT" according to [10, 18], which are employed herein to generate reference solutions

to assess the performance of L-AR schemes for the MLB model of polydisperse sedimentation. These ingredients also form the basis of the component-wise version of WENO schemes denoted "WENO-GHLL" introduced in [25], which is used to genrate the reference solution for the MMLB model.

2.1.1. *The MLB model of polydisperse sedimentation.* The MLB model of polydisperse sedimentation [24, 26] is based on the following velocity function for particles of species i (having size d_i and density ϱ_i):

$$v_i(\Phi) = v_i^{\mathrm{MLB}}(\Phi) = \mu V(\phi)\left[\delta_i(\bar{\varrho}_i - \bar{\boldsymbol{\varrho}}^{\mathrm{T}}\Phi) - \sum_{l=1}^{N}\delta_l\phi_l(\bar{\varrho}_l - \bar{\boldsymbol{\varrho}}^{\mathrm{T}}\Phi)\right], \quad i = 1,\dots,N. \tag{2.2}$$

Here $\mu = gd_1^2/(18\mu_{\mathrm{f}})$, where g denotes the acceleration of gravity, μ_{f} is the viscosity of the fluid, $\delta_i := d_i^2/d_1^2$, $\bar{\varrho}_i := \varrho_i - \varrho_{\mathrm{f}}$, where ϱ_{f} is the density of the fluid, $\bar{\boldsymbol{\varrho}} := (\bar{\varrho}_1,\dots,\bar{\varrho}_N)^{\mathrm{T}}$, and $V(\phi)$ is a so-called hindered settling factor, which is a given function $V = V(\phi)$ of the total solids volume fraction $\phi := \phi_1 + \cdots + \phi_N$ that is assumed to satisfy

$$V(0) = 1, \quad V'(\phi) \le 0 \quad \text{for } 0 \le \phi \le \phi_{\max}, \quad V(\phi_{\max}) = 0. \tag{2.3}$$

For equal-density particles, we have $\varrho_i =: \varrho_{\mathrm{s}}$ for $i = 1,\dots,N$. We define $\boldsymbol{\delta} := (\delta_1,\delta_2,\dots,\delta_N)^{\mathrm{T}}$, $\delta_1 = 1$. Then (2.2) reduces to

$$v_i(\Phi) = \mu(\varrho_{\mathrm{s}} - \varrho_{\mathrm{f}})V(\phi)(1-\phi)(\delta_i - \boldsymbol{\delta}^{\mathrm{T}}\Phi). \tag{2.4}$$

Since $\phi_{\max} \le 1$, the function $\phi \mapsto V(\phi)(1-\phi)$ satisfies (2.3), we may absorb $(\varrho_{\mathrm{s}} - \varrho_{\mathrm{f}})$ into the constant μ and the factor $(1-\phi)$ into $V(\phi)$ to obtain the following simplified equation instead of (2.4):

$$v_i(\Phi) = \mu V(\phi)(\delta_i - \boldsymbol{\delta}^{\mathrm{T}}\Phi). \tag{2.5}$$

A common expression for $V(\phi)$ appearing in (2.5) is the Richardson-Zaki [27] formula

$$V(\phi) = \begin{cases} (1-\phi)^{n_{\mathrm{RZ}}} & \text{for } 0 \le \phi \le \phi_{\max}, \\ 0 & \text{for } \phi > \phi_{\max}, \end{cases} \tag{2.6}$$

where $n_{\mathrm{RZ}} \ge 2$ is a material specific exponent. Clearly, (2.5) is a case of (2.1) for $m = 2$ with $p_1(\Phi) = \phi$ and $p_2(\Phi) = \boldsymbol{\delta}^{\mathrm{T}}\Phi$. Moreover, $v_1 \ge 0$ (since $\delta_1 - \boldsymbol{\delta}^{\mathrm{T}}\Phi = 1 - \boldsymbol{\delta}^{\mathrm{T}}\Phi \ge 0$), but $v_2,\dots,v_N$ may have either sign. The following theorem, proved in [18], is relevant for the present numerical methods and for the construction of WENO-SPEC-INT schemes in this case. Here $\mathcal{D}^0_{\phi_{\max}}$ denotes the interior of the set $\mathcal{D}_{\phi_{\max}}$ defined in (1.5).

Theorem 2.1 (Interlacing property of MLB model [18])**.** *If $\delta_1 > \delta_2 > \cdots > \delta_N$ and $\Phi \in \mathcal{D}^0_{\phi_{\max}}$, then the system* (1.1) *with $\boldsymbol{f}(\Phi)$ defined by* (1.2) *and* (2.5)*, where the function V is assumed to satisfy* (2.3)*, is strictly hyperbolic, i.e., $\mathcal{J}_{\boldsymbol{f}}(\Phi)$ has N distinct real eigenvalues $\lambda_1,\dots,\lambda_N$. Precisely, the following so-called interlacing property holds, where $\gamma_i = \mu(V'(\phi)(1-\phi) - V(\phi))\delta_i\phi_i$ for $i = 1,\dots,N$:*

$$v_1 > \lambda_1 > v_2 > \lambda_2 > \cdots > v_N > \lambda_N > M_1 := v_N + \gamma_1 + \cdots + \gamma_N.$$

2.1.2. *The modified MLB model (MMLB model) of polydisperse sedimentation.* Under fairly general conditions, the exponent n_{RZ} appearing in (2.6) is a decreasing function of the ratio between particle size and vessel diameter [27]. Based on this observation, Basson et al. [2] proposed to improve the agreement of the MLB model with experimental results by using, instead of (2.5), (2.6), the formula

$$v_i(\Phi) = \mu V_i(\phi)(\delta_i - \boldsymbol{\delta}^{\mathrm{T}}\Phi), \quad \text{where} \quad V_i(\phi) = \begin{cases} (1-\phi)^{n_{\mathrm{RZ},i}} & \text{for } 0 \le \phi \le \phi_{\max}, \\ 0 & \text{for } \phi > \phi_{\max}, \end{cases} \tag{2.7}$$

which defines the so-called modified MLB model (MMLB model). Again, $v_1 \ge 0$ but the velocities $v_2,\dots,v_N$ may have either sign. In this case the following hyperbolicity result holds.

Theorem 2.2 (Interlacing property of MMLB model [9])**.** *If $\delta_1 > \delta_2 > \cdots > \delta_N$ and $\Phi \in \mathcal{D}^0_{\phi_{\max}}$, then the system* (1.1) *with $\boldsymbol{f}(\Phi)$ defined by* (2.7)*, where the exponents $n_{\mathrm{RZ},i}$ are assumed to satisfy $n_{\mathrm{RZ},1} \le n_{\mathrm{RZ},2} \le$*

$\cdots \le n_{\mathrm{RZ},N}$, is strictly hyperbolic, i.e., $\mathcal{J}_{\boldsymbol{f}}(\Phi)$ has N distinct real eigenvalues $\lambda_1, \ldots, \lambda_N$. Precisely, the following so-called interlacing property holds, where $\gamma_i = \mu(V_i'(\phi)(1-\phi) - V_i(\phi))\delta_i\phi_i$ for $i = 1, \ldots, N$:

$$v_1 > \lambda_1 > v_2 > \lambda_2 > \cdots > v_N > \lambda_N > M_1 := v_N + \gamma_1 + \cdots + \gamma_N.$$

Note that Theorem 2.1 is not a special case of Theorem 2.2, since Theorem 2.1 also applies to functions V given in other forms than (2.6).

2.1.3. *The Davis and Gecol model of polydisperse sedimentation.* Batchelor [3] postulated that in a dilute suspension, the phase velocity v_i of spheres of species i (having diameter d_i) can be approximated by

$$v_i(\Phi) = \mu\delta_i(1 + \boldsymbol{e}_i^{\mathrm{T}}\boldsymbol{S}\Phi), \quad i = 1, \ldots, N, \tag{2.8}$$

where $\boldsymbol{e}_i$ is the N-dimensional vector having the entries one at position i and zero otherwise, $\boldsymbol{S} = (S_{ij})_{1\le i,j\le N}$ is the matrix of the so-called Batchelor coefficients. For equal-density spheres, the entries of $\boldsymbol{S}$ depend on the diameter ratios and are given for several special cases by Batchelor and Wen [4]. A common approach is

$$S_{ij} = \sum_{l=0}^{3} \beta_l \left(\frac{d_j}{d_i}\right)^l, \quad 1 \le i, j \le N \tag{2.9}$$

with non-positive coefficients $\boldsymbol{\beta} = (\beta_0, \ldots, \beta_3)^{\mathrm{T}}$. We here limit the discussion to the numerical values

$$\boldsymbol{\beta} = (-3.52, -1.04, -1.03, 0)^{\mathrm{T}} \tag{2.10}$$

that fit data obtained in [4] for large Péclet numbers to a second-order polynomial in particle size ratio [9].

Inserting $v_i(\Phi)$ defined by (2.8) into (1.2) produces a set of governing equations (1.1) that describes the settling process in the dilute limit $\Phi \to \mathbf{0}$. The first attempt to convert (2.8) into a well-defined formula for all Φ, but which agrees with (2.8) as $\Phi \to \mathbf{0}$, was made by Davis and Gecol [15], who proposed

$$v_i(\Phi) = \mu\delta_i V_i(\phi)\left(1 + \sum_{l=1}^{N}(S_{il} - S_{ii})\phi_l\right), \quad \text{where} \quad V_i(\phi) = \begin{cases} (1-\phi)^{-S_{ii}} & \text{for } 0 \le \phi \le \phi_{\max}, \\ 0 & \text{for } \phi > \phi_{\max}. \end{cases} \tag{2.11}$$

Note that these velocity functions also have variable sign in general. For example, for the case $N = 2$ and $d_2/d_1 = 1/2$ and the coefficients (2.10) we obtain

$$v_1(\phi_1, \phi_2) = \mu(1-\phi)^{3.52}(1 + 0.9325\phi_2), \quad v_2(\phi_1, \phi_2) = 0.25\mu(1-\phi)^{3.52}(1 - 4.13\phi_1),$$

so v_2 changes sign across $\phi_1 = 1/4.13 \approx 0.2421$.

It was shown in [13] that for the case $N = 2$, the Davis-Gecol (DG) model resulting from utilizing (2.11) in (1.2) is hyperbolic only for equal-density spheres that differ in size by a factor of at most about five; otherwise, unrealistic ellipticity (instability) regions emerge. For coefficients $\beta_0, \beta_1, \beta_2 < 0$, $\beta_3 = 0$ and $\beta_0, \ldots, \beta_3 < 0$, the DG model (2.11) with coefficients S_{ij} defined by (2.9) corresponds to the case $m = 3$ and $m = 4$ of (2.1), respectively, since in each case by (2.9), the formula for v_i depends on m independent linear combinations of $\phi_1, \ldots, \phi_N$ [9]. For general N it has been possible to estimate the hyperbolicity region of the DG model [11] in terms of $\phi_{\max}$ and the width of the particle size distribution expressed by the smallest particle size ratio $\delta_N^{1/2} = d_N/d_1$. The approximate hyperbolicity analysis of the DG model, conducted in [11] by the secular equation approach [1, 18] is outside the scope of the paper; however, in the numerical examples the parameters of the DG model have been chosen in such a way that hyperbolicity is ensured.

2.2. **Two simple difference schemes for the polydisperse sedimentation model** [12]**.** If $\Delta x = L/M$ denotes a spatial meshsize, $x_j = (j-1/2)\Delta x$ for $j = 1, \ldots, M$, $\Delta t > 0$ is a time step, $t^n := n\Delta t$, $\lambda := \Delta t/\Delta x$, and ϕ_{ij}^n denotes the approximate cell average of ϕ_i on the cell $[x_{j-1/2}, x_{j+1/2}] \times [t^n, t^{n+1})$, then the interior

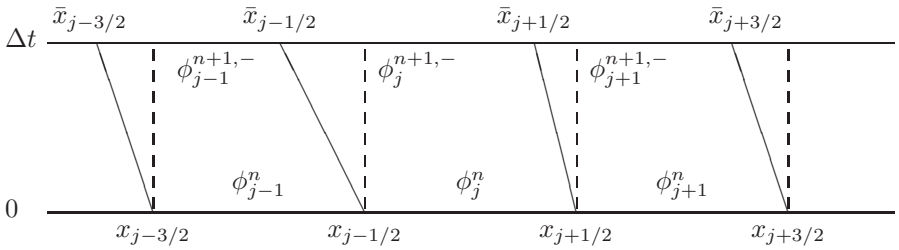

FIGURE 1. Illustration of the Lagrangian step with non-positive velocities.

version of Scheme 8 of [12] is defined by

$$\begin{aligned} \phi_{ij}^{n+1} &= \phi_{ij}^n - \lambda\big(h_i(\Phi_j^n, \Phi_{j+1}^n) - h_i(\Phi_{j-1}^n, \Phi_j^n)\big), \\ h_i(\Phi_j^n, \Phi_{j+1}^n) &:= \frac{1}{2}\big(\phi_{i,j+1}^n v_i(\Phi_{j+1}^n) + \phi_{ij}^n v_i(\Phi_j^n)\big) - \frac{E_{j+1}}{2}\big(\phi_{i,j+1}^n - \phi_{ij}^n\big) \\ &\quad - \frac{\phi_{ij}^n}{2}\big|v_i(\Phi_j^n) - v_i(\Phi_{j+1}^n)\big|\,\mathrm{sgn}(\phi_{i,j+1}^n - \phi_{ij}^n), \quad i = 1,\dots,N, \quad j = 1,\dots,M, \end{aligned} \tag{2.12}$$

which defines Scheme 8, and where $E_{j+1} := \max\{|v_1(\Phi_{j+1}^n)|, \dots, |v_N(\Phi_{j+1}^n)|\}$. Scheme 10 of [12] is a version of (2.12) that is second-order accurate both in space and time. It is based on MUSCL-type spatial differencing and Runge-Kutta (RK) time stepping. The MUSCL version of $h_i(\cdot,\cdot)$ is given by

$$h_i^{\mathrm{MUSCL}}\big(\Phi_{j-1}^n, \dots, \Phi_{j+2}^n\big) = h_i\left(\Phi_j^n + \frac{1}{2}\boldsymbol{\sigma}_j^n, \Phi_{j+1}^n - \frac{1}{2}\boldsymbol{\sigma}_{j+1}^n\right), \quad i = 1,\dots,N,$$

where the "slope vector" $\boldsymbol{\sigma}_j^n := (\sigma_{1,j}^n, \dots, \sigma_{N,j}^n)^{\mathrm{T}}$ is defined in terms of the van Leer [31] limiter, namely

$$\sigma_{ij}^n = \frac{|\phi_{ij}^n - \phi_{i,j-1}^n|(\phi_{i,j+1}^n - \phi_{ij}^n) + |\phi_{i,j+1}^n - \phi_{ij}^n|(\phi_{ij}^n - \phi_{i,j-1}^n)}{|\phi_{ij}^n - \phi_{i,j-1}^n| + |\phi_{i,j+1}^n - \phi_{ij}^n|}.$$

Furthermore, if we define the vector $\boldsymbol{h}^{\mathrm{MUSCL}} := (h_1^{\mathrm{MUSCL}}, \dots, h_N^{\mathrm{MUSCL}})^{\mathrm{T}}$ and

$$\boldsymbol{\Gamma}_j(\Phi_{j-2}^n, \dots, \Phi_{j+2}^n) := \lambda\big[\boldsymbol{h}^{\mathrm{MUSCL}}\big(\Phi_{j-1}^n, \dots, \Phi_{j+2}^n\big) - \boldsymbol{h}^{\mathrm{MUSCL}}\big(\Phi_{j-2}^n, \dots, \Phi_{j+1}^n\big)\big],$$

then Scheme 10 of [12] takes the following two-step form:

$$\begin{aligned} \tilde{\Phi}_j^{n+1} &= \tilde{\Phi}_j^n - \boldsymbol{\Gamma}_j\big(\Phi_{j-2}^n, \dots, \Phi_{j+2}^n\big), \\ \Phi_j^{n+1} &= \frac{1}{2}\Big(\Phi_j^n + \tilde{\Phi}_j^{n+1} - \boldsymbol{\Gamma}_j\big(\tilde{\Phi}_{j-2}^{n+1}, \dots, \tilde{\Phi}_{j+2}^{n+1}\big)\Big). \end{aligned}$$

For the ease of presentation, in the remainder of the paper we will address Schemes 8 and 10 of [12] simply as "Scheme 8" and "Scheme 10", respectively. We also recall that the "boundary versions" of Schemes 8 and 10, which handle the boundary conditions (1.4), are obtained from the corresponding interior versions by setting to zero the numerical fluxes associated with $x_{1/2}$ and $x_{M+1/2}$.

3. Lagrangian-Antidiffusive Remap (L-AR) schemes

3.1. **Spatial discretization.** The computational domain $[0, L] \times [0, T]$ is discretized as described in Section 2.2. The ratio $\lambda = \Delta t/\Delta x$ must satisfy a certain CFL condition that will be specified below. We focus first on the discretization of the scalar equation (1.6). We denote by $v_{j+1/2}^n$ an approximate value of $v(\phi)$ at the interface point $x = x_{j+1/2}$ at time t^n. To handle the boundary conditions, we extend the numerical approximations to ghost cells with the following values for $j \in \mathbb{Z}$:

$$\phi_j^n = \phi_{\max} \quad \text{for } j \le 0, \quad \text{and} \quad \phi_j^n = 0 \quad \text{for } j \ge M+1. \tag{3.1}$$

To advance the solution of (1.6) from time $t = t^n$ to $t = t^{n+1} = t^n + \Delta t$, L-AR schemes are based on splitting (1.6) into two equations, namely we first apply Lagrangian methods to solve (1.8) and use this solution as the initial condition for solving the transport equation (1.9) in a second step.

3.2. **Lagrangian step for the scalar model ($N = 1$), Case 1 ($v(\phi) < 0$, $v'(\phi) > 0$).** Defining $\tau := 1/\phi$, we obtain from (1.8) the conservation of mass equation in Lagrangian coordinates

$$\phi\partial_t\tau - \partial_x v = 0. \tag{3.2}$$

In other words, solving (1.8), or equivalently (3.2), means solving the original equation (1.6) on a moving referential mesh with velocity v. Assume now that $\boldsymbol{\phi}^n = (\phi_1^n, \dots, \phi_M^n)^{\mathrm{T}}$ is an approximate solution of (1.6) at time $t = t^n$ and used as the initial condition for (3.2). Then a numerical solution $\boldsymbol{\phi}^{n+1,-}$ of (3.2) at time Δt can be naturally computed by

$$\phi_j^{n+1,-}\big[\Delta x + \big(v_{j+1/2}^n - v_{j-1/2}^n\big)\Delta t\big] = \phi_j^n \Delta x, \quad j = 1, \dots, M, \tag{3.3}$$

or equivalently,

$$\phi_j^{n+1,-} = \frac{\phi_j^n}{1 + \lambda(v_{j+1/2}^n - v_{j-1/2}^n)}, \quad j = 1, \dots, M. \tag{3.4}$$

In fact, (3.3) states that the initial mass in the cell $[x_{j-1/2}, x_{j+1/2}]$ at time t^n (the right-hand side) equals the mass in the modified cell $[\bar{x}_{j-1/2}, \bar{x}_{j+1/2}]$ at time Δt (the left-hand side), where

$$\bar{x}_{j+1/2} = x_{j+1/2} + v_{j+1/2}^n \Delta t.$$

are the new interface positions (Figure 1). A natural choice for the velocity values in the interface points is

$$v_{j+1/2}^n := \begin{cases} v(\phi_j^n) & \text{for } j = 1, \dots, M-1, \\ 0 & \text{otherwise.} \end{cases} \tag{3.5}$$

This definition is consistent with the flux-zero boundary conditions (1.4). According to (3.1) and (3.5), we obtain that $\phi_j^{n+1,-} = \phi_{\max}$ for $j \le 0$ and $\phi_j^{n+1,-} = 0$ for $j \ge M+1$.

Note that applying the transformation $\tau_j^n = 1/\phi_j^n$ in (3.3), we obtain

$$\phi_j^n\big(\tau_j^{n+1,-} - \tau_j^n\big) = \lambda\big(v_{j+1/2}^n - v_{j-1/2}^n\big).$$

This formula illustrates that the discretization (3.3) naturally leads to a discrete version of (3.2).

The following Lemma indicates some properties of the Lagrangian scheme (3.3), (3.5).

Lemma 3.1. *Assume that the following pair of CFL conditions hold:*

$$-1 \le \lambda v(\phi_j) \le 0, \quad j = 1, \dots, M, \tag{CFL1}$$

$$0 \le \lambda\phi_{\max} v'\big(\phi_j^n\big) \le 1, \quad j = 1, \dots, M. \tag{CFL2}$$

If $\boldsymbol{\phi}_j^{n+1,-}$ is the numerical solution produced by the scheme (3.3)*, then the following properties hold.*

(*i*) *If $\phi_j^n \ge 0$ for $j = 1, \dots, M$, then $0 \le \phi_j^{n+1,-}$ for $j = 1, \dots, M$.*

(*ii*) *The following maximum property holds:*

$$\min\big\{\phi_{j-1}^n, \phi_j^n\big\} \le \phi_j^{n+1,-} \le \max\big\{\phi_{j-1}^n, \phi_j^n\big\} \quad \text{for all } j = 1, \dots, M. \tag{3.6}$$

(*iii*) *A total variation inequality for each step:*

$$\big|\phi_1^{n+1,-} - \phi_{\max}\big| + \sum_{j=2}^{M}\big|\phi_j^{n+1,-} - \phi_{j-1}^{n+1,-}\big| + \big|\phi_M^{n+1,-}\big| \le |\phi_1^n - \phi_{\max}| + \sum_{j=2}^{M}\big|\phi_j^n - \phi_{j-1}^n\big| + |\phi_M^n|. \tag{3.7}$$

Proof. Condition (CFL1) ensures that (*i*) holds. The proof of (*ii*) depends decisively on the assumption $v'(\phi) \ge 0$. Suppose that (CFL1), (CFL2) are true and $\phi_{j-1}^n \le \phi_j^n$ (the opposite case is similar). Since (3.3) can be written as

$$\phi_j^n - \phi_j^{n+1,-} = \lambda\phi_j^{n+1,-}\big(v_{j+1/2}^n - v_{j-1/2}^n\big),$$

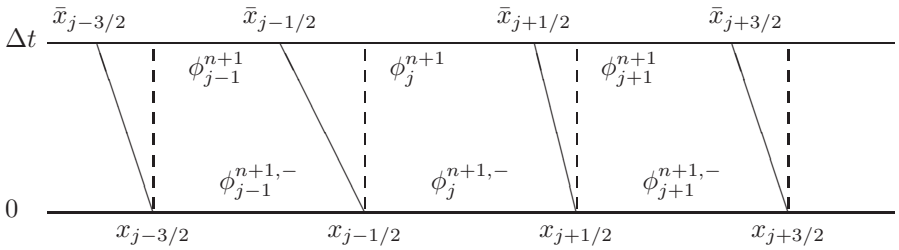

FIGURE 2. Illustration of the remap step. Note that ϕ_j^{n+1-} actually corresponds to the update formula of ϕ on the fixed mesh $[x_{j-1/2}, x_{j+1/2}]$. The remap step consists in solving a transport equation of these values with velocities $v_{j+1/2}^n$ defined at each interface $j+1/2$. The values ϕ_j^{n+1} then correspond to approximate values of ϕ, again on the fixed mesh $[x_{j-1/2}, x_{j+1/2}]$ but after a time step Δt.

according to (3.5) and the assumption on $v'(\phi)$ we obtain that $v_{j+1/2}^n \geq v_{j-1/2}^n$. In this way, we obtain $\phi_j^{n+1,-} \leq \max\{\phi_{j-1}^n, \phi_j^n\}$. On the other hand, $\phi_j^{n+1,-} \geq \phi_{j-1}^n$ is proved as soon as one can establish that

$$\frac{\phi_j^n}{1+\lambda(v_{j+1/2}^n - v_{j-1/2}^n)} \geq \phi_{j-1}^n \Leftrightarrow \big(\phi_j^n - \phi_{j-1}^n\big)\left\{1 - \lambda\phi_{j-1}^n \frac{v_{j+1/2}^n - v_{j-1/2}^n}{\phi_j^n - \phi_{j-1}^n}\right\} \geq 0.$$

However, the term in curled brackets equals $1 - \lambda\phi_{j-1}^n v'(\xi_{j-1/2}^n)$ for an intermediate value $\xi_{j-1/2}^n \in [\phi_{j-1}^n, \phi_j^n]$, and therefore is non-negative under the condition (CFL2). In particular due to boundary conditions, $\phi_1^{n+1,-} \leq \phi_{\max}$, so we obtain that $0 \leq \phi_j^{n+1,-} \leq \phi_{\max}$ for $j = 1, \ldots, M$.

Finally, to obtain (3.7) we first note that

$$\phi_j^{n+1,-} - \phi_{j-1}^{n+1,-} = \big[1 - \lambda\phi_j^{n+1,-} v'\big(\zeta_{j-1/2}^n\big)\big]\big(\phi_j^n - \phi_{j-1}^n\big) + \lambda\phi_{j-1}^{n+1,-} v'\big(\zeta_{j-3/2}^n\big)\big(\phi_{j-1}^n - \phi_{j-2}^n\big). \tag{3.8}$$

Since $\phi_j^{n+1,-} \geq 0$, $v'(\phi) \geq 0$ and

$$1 - \lambda\phi_j^{n+1,-} v'\big(\zeta_{j-1/2}^n\big) \geq 1 - \lambda\phi_{\max} v'\big(\zeta_{j-1/2}^n\big) \geq 0$$

due to (CFL2), we obtain from (3.8) that

$$\big|\phi_j^{n+1,-} - \phi_{j-1}^{n+1,-}\big| \leq \big[1 - \lambda\phi_j^{n+1,-} v'\big(\zeta_{j-1/2}^n\big)\big]\big|\phi_j^n - \phi_{j-1}^n\big| + \lambda\phi_{j-1}^{n+1,-} v'\big(\zeta_{j-3/2}^n\big)\big|\phi_{j-1}^n - \phi_{j-2}^n\big|$$

for all j. Summing over $j = 1, \ldots, M+1$, performing cancellations and considering (3.1) we get (3.7). □

3.3. **Remap step: antidiffusive scheme for the scalar model ($N = 1$), Case 1 ($v(\phi) < 0$, $v'(\phi) > 0$).** After the Lagrangian step, the new values $\phi_j^{n+1,-}$ represent approximate values of the density on a moved mesh with new cells $[\bar{x}_{j-1/2}, \bar{x}_{j+1/2}]$. To avoid dealing with moving meshes, a so-called remap step is necessary to define the new approximations ϕ_j^{n+1} on the uniform mesh with cells $[x_{j-1/2}, x_{j+1/2}]$. Figure 1 illustrates that this step amounts to "averaging" the density values at time Δt on the cells $[x_{j-1/2}, x_{j+1/2}]$. This average step can equivalently be reformulated by using the solution of the transport equation (1.9) with initial data defined by $\phi_j^{n+1,-}$ on each cell $[x_{j-1/2}, x_{j+1/2}]$, see Figure 2.

We now describe the conditions analyzed in [6] for solving the linear equation (1.9) with initial data $\boldsymbol{\phi}^{n+1,-}$ in the case where $v(\phi) \leq 0$ by using an antidiffusive numerical scheme in the form

$$\phi_j^{n+1} = \phi_j^{n+1,-} - \bar{V}_j^n \lambda\big(\phi_{j+1/2}^{n+1,-} - \phi_{j-1/2}^{n+1,-}\big), \quad j = 1, \ldots, M. \tag{3.9}$$

Here $\bar{V}_j^n < 0$ is a velocity value, defined in terms of available density values, which will be chosen in such a way that the complete scheme (3.3), (3.9) is conservative with respect to (1.6). The quantities $\phi_{j-1/2}^{n+1,-}$, $j = 1, \ldots, M$, are numerical fluxes associated with the cell interfaces $x_{j-1/2}$ and will be chosen in such a way that the scheme (3.9) has certain stability and consistency properties. In particular, the choice

$$\phi_{j-1/2}^{n+1,-} = \phi_j^{n+1,-} \quad \text{for all } j = 1, \ldots, M$$

produces a diffusive and stable scheme while

$$\phi_{j-1/2}^{n+1,-} = \phi_{j-1}^{n+1,-} \quad \text{for all } j = 1, \dots, M \tag{3.10}$$

yields an antidiffusive but unstable scheme. For this reason, Després and Lagoutière [16] (see also [6]) proposed to choose $\phi_{j-1/2}^{n+1,-}$ as close to the antidiffusive value (3.10) as possible, subject to the following constraints which resume the existence and properties of the schemes defined by (3.9), namely the consistency condition

$$m_{j-1/2} := \min\{\phi_j^{n+1,-}, \phi_{j-1}^{n+1,-}\} \le \phi_{j-1/2}^{n+1,-} \le \max\{\phi_j^{n+1,-}, \phi_{j-1}^{n+1,-}\} := M_{j-1/2}$$

and the maximum principle

$$m_{j+1/2} \le \phi_j^{n+1} \le M_{j+1/2}.$$

Let us define

$$b_j^- := M_{j+1/2} + \frac{\phi_j^{n+1,-} - M_{j+1/2}}{\max\{|v_j^n|, |v_{j-1}^n|\}\lambda}, \quad B_j^- := m_{j+1/2} + \frac{\phi_j^{n+1,-} - m_{j+1/2}}{\max\{|v_j^n|, |v_{j-1}^n|\}\lambda}$$

and

$$a_{j-1/2}^- := \max\{b_j^-, m_{j-1/2}\}, \quad A_{j-1/2}^- := \min\{B_j^-, M_{j-1/2}\},$$

and, for $a_1, \dots, a_m \in \mathbb{R}$ we define the interval $\mathcal{I}(a_1, \dots, a_m) := [\min\{a_1, \dots, a_m\}, \max\{a_1, \dots, a_m\}]$.

In the next lemma, we summarize the existence and properties of the schemes defined by (3.9).

Lemma 3.2. *If* (CFL1) *is satisfied, then* $a_{j-1/2}^- \le \phi_j^{n+1,-} \le A_{j-1/2}^-$ *for all* $j = 1, \dots, M$*, and for any flux that satisfies*

$$\phi_{j-1/2}^{n+1,-} \in [a_{j-1/2}^-, A_{j-1/2}^-] \quad \text{for all } j = 1, \dots, M, \tag{3.11}$$

the scheme (3.9) *is* L^∞*-stable, i.e.,*

$$\phi_j^{n+1} \in \mathcal{I}\big(\phi_j^{n+1,-}, \phi_{j+1}^{n+1,-}\big) \quad \text{for all } j = 1, \dots, M, \tag{3.12}$$

and the following TVD property holds:

$$\sum_{j\in\mathbb{Z}} \big|\phi_{j+1}^{n+1} - \phi_j^{n+1}\big| \le \sum_{j\in\mathbb{Z}} \big|\phi_{j+1}^{n+1,-} - \phi_j^{n+1,-}\big| \quad \text{for } n \in \mathbb{N}_0. \tag{3.13}$$

In particular, for each n *there exist numbers* $\alpha_j \in [0, 1]$ *such that*

$$\phi_j^{n+1,-} = \alpha_j \phi_{j-1/2}^{n+1,-} + (1 - \alpha_j)\phi_{j+1/2}^{n+1,-}. \tag{3.14}$$

Proof. Assume that (CFL1) holds. Then by construction it can easily be checked that

$$\phi_j^{n+1,-} \in [a_{j-1/2}^-, A_{j-1/2}^-].$$

For the proof of (3.12) and (3.13) we refer to [16]. Now, we prove (3.14). Assume that (CFL1) holds and that $\phi_{j-1/2}^{n+1,-}$ satisfies (3.11). If $\phi_j^{n+1,-} = M_{j-1/2}$, as $\phi_{j-1/2}^{n+1,-} \in [b_j^-, B_j^-]$ we obtain that

$$\phi_j^{n+1,-} \le \phi_{j-1/2}^{n+1,-} \le \max\{\phi_{j-1/2}^{n+1,-}, \phi_{j+1/2}^{n+1,-}\}. \tag{3.15}$$

On the other hand, from $\phi_{j-1/2}^{n+1,-} \in [m_{j-1/2}, M_{j-1/2}]$ we have

$$\phi_{j-1/2}^{n+1,-} \le M_{j-1/2} = \phi_j^{n+1,-},$$

and thus

$$\min\{\phi_{j-1/2}^{n+1,-}, \phi_{j+1/2}^{n+1,-}\} \le \phi_j^{n+1,-}. \tag{3.16}$$

Combining (3.15) and (3.16) we obtain $\phi_j^{n+1,-} \in \mathcal{I}(\phi_{j-1/2}^{n+1,-}, \phi_{j+1/2}^{n+1,-})$, which implies (3.14). The proof is similar if $\phi_j^{n+1,-} = m_{j-1/2}$. □

There are different ways to define the quantities $\phi_{j+1/2}^{n+1,-}$; see [6, 7, 16] and [8, Section 4.2] for non-negative velocities, but we here consider only the N-Bee method described in [6], which is well defined when velocities have variable signs. This scheme, proposed in [6] for linear transport equations (3.9) when $\bar{V}_j^n$ is a velocity function that changes sign, corresponds to a second-order scheme in space, and is constructed from the following definitions:

$$\phi_{j+1/2}^{n+1,-} = \begin{cases} \phi_{j+1/2}^{\mathrm{L}} := \phi_j^{n+1,-} + \dfrac{1-\bar{\lambda}_j}{2}\varphi^{\mathrm{NB}}(r_j, \bar{\lambda}_j)\big(\phi_{j+1}^{n+1,-} - \phi_j^{n+1,-}\big) & \text{if } \bar{V}_j > 0 \text{ and } \bar{V}_{j+1} > 0, \\ \phi_{j+1/2}^{\mathrm{R}} := \phi_{j+1}^{n+1,-} + \dfrac{1-|\bar{\lambda}_{j+1}|}{2}\varphi^{\mathrm{NB}}(r_{j+1}^-, |\bar{\lambda}_{j+1}|)\big(\phi_j^{n+1,-} - \phi_{j+1}^{n+1,-}\big) & \text{if } \bar{V}_j < 0 \text{ and } \bar{V}_{j+1} < 0, \\ \dfrac{\phi_{j+1}^{n+1,-} + \phi_j^{n+1,-}}{2} & \text{if } \bar{V}_j \cdot \bar{V}_{j+1} < 0, \end{cases} \tag{3.17}$$

where $\bar{\lambda}_j = \lambda \bar{V}_j$ and

$$r_j := \frac{\phi_j^{n+1,-} - \phi_{j-1}^{n+1,-}}{\phi_{j+1}^{n+1,-} - \phi_j^{n+1,-}}, \quad r_j^- := \frac{\phi_{j+1}^{n+1,-} - \phi_j^{n+1,-}}{\phi_j^{n+1,-} - \phi_{j-1}^{n+1,-}} = \frac{1}{r_j},$$

and the limiter function is defined as

$$\varphi^{\mathrm{NB}}(r, \bar{\lambda}) := \max\left\{0, \min\left\{1, \frac{2r}{\bar{\lambda}}\right\}, \min\left\{r, \frac{2}{1-\bar{\lambda}}\right\}\right\}.$$

It is proved in [6] that the numerical flux that corresponds to the second of the alternatives in (3.17) satisfies the assumptions of Lemma 3.2.

3.4. **Lagrangian-antidiffusive remap (L-AR) schemes for the scalar model ($N = 1$), Case 1 ($v(\phi) < 0$, $v'(\phi) > 0$).** Assume that $\boldsymbol{\phi}^n$ approximates the solution of (1.6) at time $t = t^n$ and we wish to advance this solution to $t = t^{n+1} = t^n + \Delta t$. To this end, two steps are performed successively:

(1) *Lagrangian step.* Consider that $\boldsymbol{\phi}^n$ is an initial solution for (1.8). First, we define the intermediate velocities $v_{j+1/2}^n$ according to the assumption on $v'(\phi)$, in this case, we use formula (3.5). Then we compute the numerical solution $\boldsymbol{\phi}^{n+1,-}$ of equation (1.8) after an evolution over a time interval of length Δt, by using scheme (3.3).

(2) *Antidiffusive remap step.* Solve (1.9) with initial condition $\boldsymbol{\phi}^{n+1,-}$ using an antidiffusive scheme (3.9) for a specific choice of $\bar{V}_j^n$, obtaining a numerical solution $\boldsymbol{\phi}^{n+1}$ which approximates the solution of (1.6) at time $t = t^{n+1}$.

In the next theorem, the choice of $\bar{V}_j^n$ is motivated by the existence of a classical conservative update formula for the whole L-AR scheme (3.3), (3.9).

Theorem 3.1. *Under conditions* (CFL1) *and* (CFL2) *there exists a definition of* $\bar{V}_j^n \in \mathcal{I}(v_{j-1/2}^n, v_{j+1/2}^n)$ *such that the complete L-AR scheme can be written in the form*

$$\phi_j^{n+1} = \phi_j^n - \lambda\big(\phi_{j+1/2}^{n+1,-} v_{j+1/2}^n - \phi_{j-1/2}^{n+1,-} v_{j-1/2}^n\big), \quad j \in \mathbb{Z}_M, \quad n \in \mathbb{N}_0. \tag{3.18}$$

Proof. Let $\boldsymbol{\phi}^{n+1,-}$ be a solution of (1.8) obtained by scheme (3.3). Using this solution we solve (1.9) by the scheme (3.9), where the value $\bar{V}_j^n$ still needs to be determined in such a way that the resulting scheme is conservative. Replacing $\phi_j^{n+1,-}$ in (3.9) by

$$\phi_j^{n+1,-} = \phi_j^n - \lambda\big(v_{j+1/2}^n - v_{j-1/2}^n\big)\phi_j^{n+1,-},$$

we obtain

$$\phi_j^{n+1} = \phi_j^n - \lambda \bar{V}_j^n\big(\phi_{j+1/2}^{n+1,-} - \phi_{j-1/2}^{n+1,-}\big) - \lambda\big(v_{j+1/2}^n - v_{j-1/2}^n\big)\phi_j^{n+1,-}. \tag{3.19}$$

Since $\phi_{j-1/2}^{n+1,-}$ satisfies the assumptions of Lemma 3.2, (3.14) says that there exist $\alpha_j \in [0,1]$ such that

$$\phi_j^{n+1,-} = \alpha_j \phi_{j-1/2}^{n+1,-} + (1-\alpha_j)\phi_{j+1/2}^{n+1,-} \quad \text{for } j = 1, \ldots, M.$$

Setting $\bar{V}_j^n := (1-\alpha_j)v_{j-1/2}^n + \alpha_j v_{j+1/2}^n$ and replacing in (3.19) we obtain (3.18). □

Note that the numerical scheme (3.18) is written in conservative form as

$$\phi_j^{n+1} = \phi_j^n - \lambda\big(F_{j+1/2}^n - F_{j-1/2}^n\big), \tag{3.20}$$

where the numerical flux in the case is given in the case $v < 0$, $v' > 0$ by

$$F_{j+1/2}^n := F\big(\phi_{j-1}^n, \dots, \phi_{j+2}^n\big) := \phi_{j+1/2}^{\mathrm{R}} v_j^n.$$

This four-point numerical flux is consistent with the flux $f(\phi) = \phi v(\phi)$ since by (3.3) and (3.6), we have $\phi_{j-1}^{n+1,-}, \phi_j^{n+1,-}, \phi_{j+1}^{n+1,-} \to \phi$ as $\phi_{j-1}^n, \dots, \phi_{j+2}^n \to \phi$. This eventually means that $F(\phi, \dots, \phi) = \phi v(\phi)$.

Next, we prove some properties of the numerical scheme (3.18).

Theorem 3.2. *Under conditions* (CFL1) *and* (CFL2) *the numerical scheme* (3.18) *has the TVD property, is L^∞-stable, and as a consequence of* (3.6) *and* (3.12) *it satisfies $\phi_j^{n+1} \in \mathcal{I}(\phi_{j-1}^n, \phi_j^n, \phi_{j+1}^n)$ for all j and $n \in \mathbb{N}_0$.*

Proof. We recall from Lemma 3.2 that if (CFL1) is satisfied and the scheme associated with the remap step, (3.9), satisfies (3.11), then (3.9) has the TVD property (3.13). Then, (3.13) and (3.7) imply that (3.18) is TVD under conditions (CFL1) and (CFL2). The L^∞ bound is a standard consequence of the TVD property. □

Remark 3.1. *Theorem 3.2 implies that under conditions* (CFL1) *and* (CFL2) *and if $\phi_0 \in L^1(\mathbb{R})$, the numerical solution of scheme* (3.18) *converges in $L^\infty([0,T], L^1_{\mathrm{loc}})$ to a weak solution of* (1.6)*, see* [19].

3.5. **L-AR schemes for the scalar model ($N = 1$), Case 2 ($v(\phi) \geq 0$, $v'(\phi) \leq 0$).** In [8] L-AR schemes for the scalar model and Case 2 were proposed. In that case, the Lagrangian step is obtained using formula (3.3), where $v_{j+1/2}^n$ is computed by

$$v_{j+1/2}^n = v\big(\phi_{j+1}^n\big) \quad \text{for } j = 1, \dots, M.$$

Note that this definition is different from that of the case $v(\phi) < 0$ and $v'(\phi) > 0$, see (3.5). The remap step is solved by using an antidiffusive scheme (3.9) where the quantities $\phi_{j+1/2}^{n+1,-}$ are calculated using the NBee scheme defined by the first alternative in (3.17). The resulting scheme can be written in conservative form (3.20) with numerical flux

$$F_{j+1/2}^n := F\big(\phi_{j-1}^n, \dots, \phi_{j+2}^n\big) := \phi_{j+1/2}^{\mathrm{L}} v_{j+1}^n.$$

Analogues of Lemmas 3.1 and 3.2 and Theorem 3.2 for non-negative velocities are proved in [8].

3.6. **L-AR schemes for the scalar model ($N = 1$), Case 3 ($v(\phi)$ and $v'(\phi)$ with variable sign).** For Case 3, the discussion of Cases 1 and 2 motivates us to redefine the intermediate velocities according to the sign of $v'(\phi)$ as

$$v_{j+1/2}^n = \begin{cases} v(\phi_j^n) & \text{if } (v(\phi_{j+1}^n) - v(\phi_j^n))(\phi_{j+1}^n - \phi_j^n) > 0, \\ v(\phi_{j+1}^n) & \text{if } (v(\phi_{j+1}^n) - v(\phi_j^n))(\phi_{j+1}^n - \phi_j^n) \leq 0. \end{cases} \tag{3.21}$$

Based on the values $v_{j+1/2}^n$ defined by (3.21) we compute the numerical solution $\boldsymbol{\phi}^{n+1,-}$ of the Lagrangian step by using formula (3.3) and then, the numerical fluxes as

$$F_{j+1/2}^n := \phi_{j+1/2}^{\mathrm{L}} \max\big\{0, v_{j+1/2}^n\big\} + \phi_{j+1/2}^{\mathrm{R}} \min\big\{0, v_{j+1/2}^n\big\}, \tag{3.22}$$

where $\phi_{j+1/2}^{\mathrm{L}}$ and $\phi_{j+1/2}^{\mathrm{R}}$ are the intermediate N-Bee fluxes defined in (3.17).

Now if $\boldsymbol{\phi}^n$ is an approximation of $\phi(\cdot, t^n)$ in the sense of a finite volume scheme, we can compute $\boldsymbol{\phi}^{n+1}$ in three steps as follows.

(1) Compute $v_{j+1/2}^n$ according to (3.21) for $j = 0, \dots, M$.
(2) Compute $\boldsymbol{\phi}^{n+1,-}$ by the Lagrangian step (3.4).
(3) Calculate the intermediate fluxes $\phi_{j+1/2}^{\mathrm{L}}$ and $\phi_{j+1/2}^{\mathrm{R}}$, $j = 0, \dots, M$, by the NBee scheme (3.17), and compute the corresponding numerical fluxes $F_{j+1/2}^n$ by (3.22). Compute the numerical solution at t^{n+1}, namely $\boldsymbol{\phi}^{n+1}$, by the conservative scheme

$$\phi_j^{n+1} = \phi_j^n - \lambda\big(F_{j+1/2}^n - F_{j-1/2}^n\big), \quad j = 1, \dots, M. \tag{3.23}$$

To demonstrate that the resulting scheme has properties analogous to those established for Cases 1 and 2 of a scalar equation, we limit the discussion to velocity functions $v(\phi)$ that satisfy the following assumption.

Assumption 3.1. *The velocity function $v(\phi)$ satisfies $v(\phi_{\max}) = 0$ and there exists precisely one value $\phi^* \in (0, \phi_{\max})$ such that $v'(\phi) \le 0$ for $0 \le \phi \le \phi^*$ and $v'(\phi) > 0$ for $\phi^* < \phi \le \phi_{\max}$.*

Theorem 3.3. *Assume that $v(\phi)$ satisfies Assumption 3.1 and the following pair of CFL conditions hold:*

$$\lambda |v(\phi_j)| \le \frac{1}{2}, \quad j \in \mathbb{Z}, \tag{CFL3}$$

$$\lambda \phi_{\max} |v'(\phi_j^n)| \le 1, \quad j \in \mathbb{Z}. \tag{CFL4}$$

If $\boldsymbol{\phi}_j^{n+1,-}$ is the numerical solution produced by the Lagrangian step (3.4)*, then the following properties hold.*

(i) If $\phi_j^n \ge 0$ for $j = 1, \dots, M$, then $\phi_j^{n+1,-} \ge 0$ for $j = 1, \dots, M$.

(ii) The following maximum property holds:

$$\phi_j^{n+1,-} \in \mathcal{I}(\phi_{j-1}^n, \phi_j^n, \phi_{j+1}^n) \quad \text{for all } j = 1, \dots, M. \tag{3.24}$$

(iii) The total variation bound (3.7) *remains in effect.*

Proof. First of all, we remark that (i) is a direct consequence of (CFL3). We assume that $v(\phi)$ satisfies Assumption 3.1 and suppose, without loss of generality, that there exists $k \in \{1, \dots, M\}$ such that

$$\operatorname{sgn}\Big(\big(v(\phi_{j+1}^n) - v(\phi_j^n)\big)\big(\phi_{j+1}^n - \phi_j^n\big) \Big) \begin{cases} \le 0 & \text{for } j < k-1, \\ > 0 & \text{for } j \ge k. \end{cases}$$

In this way, the intermediate velocities computed by (3.21) satisfy

$$v_{j+1/2}^n = \begin{cases} v(\phi_{j+1}^n) & \text{for } j \le k-1, \\ v(\phi_j^n) & \text{for } j \ge k. \end{cases}$$

After the Lagrangian step, we obtain

$$\phi_j^{n+1,-} = \begin{cases} \dfrac{\phi_j^n}{1 + \lambda(v(\phi_{j+1}^n) - v(\phi_j^n))} & \text{for } j \le k-1, \\ \phi_j^n & \text{for } j = k, \\ \dfrac{\phi_j^n}{1 + \lambda(v(\phi_j^n) - v(\phi_{j-1}^n))} & \text{for } j \ge k-1. \end{cases}$$

Assuming that (CFL4) holds, we obtain from [8, Lemma 3.1 and Remark 3.1] the following inclusions, which imply (3.24):

$$\phi_j^{n+1,-} \begin{cases} \in \mathcal{I}(\phi_j^n, \phi_{j+1}^n) & \text{for } j < k, \\ \in \mathcal{I}(\phi_{j-1}^n, \phi_j^n) & \text{for } j > k. \end{cases}$$

To prove the total variation inequality observe that from [8, (4.15)] we have

$$\big|\phi_{j+1}^{n+1,-} - \phi_j^{n+1,-}\big| \le \big[1 + \lambda \phi_j^{n+1,-} v'(\xi_{j+1/2}^n)\big] \big|\phi_{j+1}^n - \phi_j^n\big| - \lambda \phi_{j+1}^{n+1,-} v'(\xi_{j+3/2}^n) \big|\phi_{j+2}^n - \phi_{j+1}^n\big| \quad \text{for } j \le k-2$$

and by (3.8) in the proof of Lemma 3.1,

$$\big|\phi_{j+1}^{n+1,-} - \phi_j^{n+1,-}\big| \le \big[1 - \lambda \phi_{j+1}^{n+1,-} v'(\xi_{j+1/2}^n)\big] \big|\phi_{j+1}^n - \phi_j^n\big| + \lambda \phi_j^{n+1,-} v'(\xi_{j-1/2}^n) \big|\phi_j^n - \phi_{j-1}^n\big| \quad \text{for } j \ge k+1$$

for suitable values $\xi_{j+1/2}^n \in \mathcal{I}(\phi_j^n, \phi_{j+1}^n)$. On the other hand,

$$\phi_k^{n+1,-} - \phi_{k-1}^{n+1,-} = \phi_k^n - \phi_{k-1}^n + \lambda \phi_{k-1}^{n+1,-} v'(\xi_{k-1/2}^n)\big(\phi_k^n - \phi_{k-1}^n\big)$$

and

$$\phi_{k+1}^{n+1,-} - \phi_k^{n+1,-} = \phi_{k+1}^n - \phi_k^n - \lambda \phi_{k+1}^{n+1,-} v'(\xi_{k+1/2}^n)\big(\phi_{k+1}^n - \phi_k^n\big).$$

Summing over $j = 0, \dots, M$ and performing appropriate cancellations we get (3.7). □

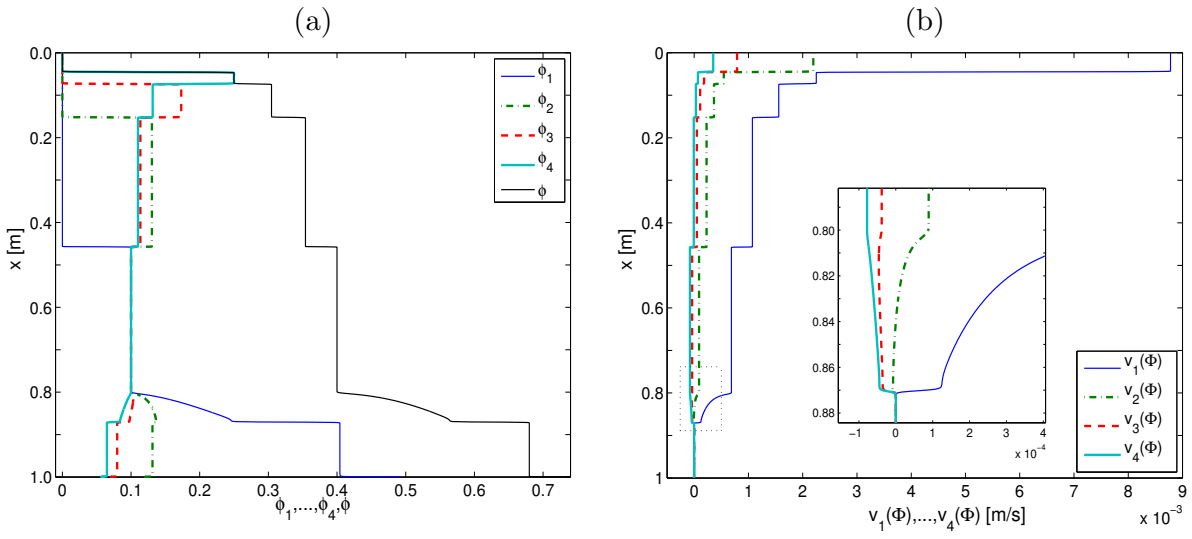

FIGURE 3. Numerical solution of the MLB model $N = 4$ for normalized diameters $(d_1, d_2, d_3, d_4) = (1.0, 0.5, 0.3, 0.2)$, $V(\phi)$ given by (2.6) with $n_{\mathrm{RZ}} = 4.7$ and $\Phi^0 = (0.1, 0.1, 0.1, 0.1)^{\mathrm{T}}$, showing (a) the solution Φ at simulated time $T = 200$s and (b) the velocity v_i of each species at that time obtained by evaluating (2.5) with the numerical approximation of Φ.

Concerning the remap step, we employ the scheme (3.9) where the intermediate fluxes $\phi^{n+1,-}_{j+1/2}$ are calculated by the NBee scheme (as stated above). It is proved in [6, Prop. 4.1] that the numerical scheme (3.9) under the CFL condition $\lambda|\bar{V}^n_j| < 1$ for all j is consistent, L^∞-stable and TVD.

Theorem 3.4. *Under conditions* (CFL3) *and* (CFL4) *there exists a definition of* $\bar{V}^n_j \in \mathcal{I}(v^n_{j-1/2}, v^n_{j+1/2})$ *such that the complete L-AR scheme can be written in the form* (3.22), (3.23), *In this case we obtain* $\lambda|\bar{V}^n_j| < 1$ *for all* j *and, as a consequence of* [6, Th. 1] *and* [6, Prop. 4.1], *the numerical scheme* (3.22), (3.23) *is consistent, L^∞-stable and TVD.*

3.7. **Definition of L-AR schemes for $N > 1$.** In polydisperse sedimentation models for $N > 1$ we know that some velocities can be negative or can change sign and $v_i(\Phi) \longrightarrow 0$ as $\phi \to \phi_{\max}$, but no analogue of the sign of $v'(\phi)$ evaluated in the scalar case is known. In Figure 3 we plot as an example a solution of the MLB model for $N = 4$ that illustrates that negative velocities indeed occur in standard situations. Consequently, for the implementation of L-AR schemes for polydisperse sedimentation models it is natural to define the intermediate velocities $v^n_{i,j+1/2}$, $i = 1, \ldots, N$, by applying (3.21) in a component-wise manner, giving rise to

$$v^n_{i,j+1/2} = \begin{cases} v_i(\Phi^n_j) & \text{if } (v_i(\Phi^n_{j+1}) - v_i(\Phi^n_j))(\phi^n_{i,j+1} - \phi^n_{ij}) > 0, \\ v_i(\Phi^n_{j+1}) & \text{if } (v_i(\Phi^n_{j+1}) - v_i(\Phi^n_j))(\phi^n_{i,j+1} - \phi^n_{ij}) \le 0, \end{cases} \quad i = 1, \ldots, N. \tag{3.25}$$

Based on (3.25), Lagrangian values $\phi^{n+1,-}_{i,j}$ are computed by considering (3.3) for each component, i.e.,

$$\phi^{n+1,-}_{i,j}\big[\Delta x + \big(v^n_{i,j+1/2} - v^n_{i,j-1/2}\big)\Delta t\big] = \phi^n_{ij}\Delta x, \quad i = 1, \ldots, N. \tag{3.26}$$

Finally, the numerical fluxes are given by

$$F^n_{i,j+1/2} := \phi^{\mathrm{L}}_{i,j+1/2} \max\big\{v^n_{i,j+1/2}, 0\big\} + \phi^{\mathrm{R}}_{i,j+1/2} \min\big\{v^n_{i,j+1/2}, 0\big\}, \quad i = 1, \ldots, N, \quad j = 0, \ldots, M, \tag{3.27}$$

where $\phi^{\mathrm{L}}_{i,j+1/2}$ and $\phi^{\mathrm{R}}_{i,j+1/2}$ are computed according to (3.17) in each component. Thus, we refer to the *L-NBee scheme* for $N > 1$ as the numerical scheme (3.20) applied in a component-wise manner, with intermediate velocities (3.25), Lagrangian values $\phi^{n+1,-}_{i,j}$ as in (3.26), and numerical fluxes (3.27).

3.8. **L-AR schemes with improved accuracy by MUSCL-type extrapolation ($N > 1$).** A standard device to upgrade a conservative difference scheme to second-order accuracy in space is MUSCL-type variable extrapolation [32, 33]. To implement it, we approximate $\phi(x, t^n)$ by a piecewise linear numerical solution in each cell, i.e., $\hat{\phi}_j(x, t^n) = \phi_j^n + \sigma_j^n(x - x_j)$, where the slopes σ_j^n are calculated via the standard minmod function, i.e.,

$$\sigma_j^n = \frac{1}{\Delta x}\operatorname{minmod}\big(\phi_j^n - \phi_{j-1}^n, \phi_{j+1}^n - \phi_j^n\big), \quad \text{where } \operatorname{minmod}(a,b) = \begin{cases} \operatorname{sgn}(a)\min\{|a|,|b|\} & \text{if } \operatorname{sgn} a = \operatorname{sgn} b, \\ 0 & \text{otherwise.} \end{cases}$$

This extrapolation enables one to define left and right values defined by

$$\begin{aligned} \phi_{j+1/2,\mathrm{L}}^n &:= \hat{\phi}_j^n\left(x_j + \frac{\Delta x}{2}\right), \quad v_{j+1/2}^{\mathrm{L}} := v\big(\phi_{j+1/2,\mathrm{L}}^n\big), \\ \phi_{j+1/2,\mathrm{R}}^n &:= \hat{\phi}_{j+1}\left(x_{j+1} - \frac{\Delta x}{2}\right), \quad v_{j+1/2}^{\mathrm{R}} := v\big(\phi_{j+1/2,\mathrm{R}}^n\big), \quad j = 1, \ldots, M. \end{aligned} \tag{3.28}$$

Equations (3.28) can be applied in a component-wise manner. Then for $N > 1$ we define intermediate velocities according to the formula

$$v_{i,j+1/2}^n = \begin{cases} v_{i,j+1/2}^{\mathrm{L}} & \text{if } (v_{i,j+1/2}^{\mathrm{R}} - v_{i,j+1/2}^{\mathrm{L}})(\phi_{j+1/2,\mathrm{R}}^n - \phi_{j+1/2,\mathrm{L}}^n) > 0, \\ v_{i,j+1/2}^{\mathrm{R}} & \text{if } (v_{i,j+1/2}^{\mathrm{R}} - v_{i,j+1/2}^{\mathrm{L}})(\phi_{j+1/2,\mathrm{R}}^n - \phi_{j+1/2,\mathrm{L}}^n) \le 0. \end{cases} \tag{3.29}$$

After that, Lagrangian values $\phi_{i,j}^{n+1,-}$ are computed as in (3.26) with $v_{i,j+1/2}^n$ as in (3.29) and the numerical fluxes (3.27). Next we compute $\phi_{i,j+1/2}^{\mathrm{L}}$ and $\phi_{i,j+1/2}^{\mathrm{R}}$ as in (3.17) and finally the numerical fluxes (3.27). This results in

$$F_{i,j+1/2}^n := \phi_{i,j+1/2}^{\mathrm{L}} \max\big\{v_{i,j+1/2}^{\mathrm{R}}, 0\big\} + \phi_{i,j+1/2}^{\mathrm{R}} \min\big\{v_{i,j+1/2}^{\mathrm{L}}, 0\big\}, \quad i = 1, \ldots, N, \quad j = 1, \ldots, M. \tag{3.30}$$

From now on, we address as L-NBee-MUSCL scheme the numerical scheme (3.20) applied in a component-wise manner with intermediate velocities (3.29), Lagrangian values $\phi_{i,j}^{n+1,-}$ as in (3.26), and numerical fluxes (3.30). Observe that this scheme is only a single-step scheme in time.

4. Numerical results

In the subsequent series of examples, we solve system (1.1) numerically for $0 \le t \le T$ and $0 \le x \le L$ and start in each case from a suspension with an initially homogeneous composition, i.e., $\Phi_0(x) = \Phi^0 \in \mathcal{D}_{\phi_{\max}}$ for $x \in [0, L]$. We compare the numerical results obtained by the L-NBee scheme with those obtained from Schemes 8 and 10 described in Section 2.2 and the WENO-SPEC-INT scheme introduced in [10]. For all schemes, Δt is selected in each time step according to

$$\Delta t = \frac{\Delta x}{2}\Big(\max_{i=1,\ldots,N}\max_{\Phi\in\mathcal{D}_{\phi_{\max}}} |v_i(\Phi)|\Big)^{-1}.$$

Examples 1 and 2 address the scalar case ($N = 1$) that permits the construction of an exact entropy weak solution, while Examples 3 to 6, where $N > 1$, involve the computation of a reference solution to compute approximate errors. These reference solutions are computed by the WENO-SPEC-INT scheme with $M_{\mathrm{ref}} = 25600$ cells. Total approximate L^1 errors at different times for each scheme are computed as follows. Let us denote by $(\phi_{j,i}^M(t))_{j=1}^M$ and $(\phi_{l,i}^{\mathrm{ref}}(t))_{l=1}^{M_{\mathrm{ref}}}$ the numerical solution for the i-th component at time t calculated with M and M_{ref} cells, respectively. We use cubic interpolation from the reference grid to the M cells grid to compute $\widetilde{\phi}_{j,i}^{\mathrm{ref}}(t)$ for $j = 1, \ldots, M$. We calculate the approximate L^1 error in species i by

$$e_i(t) := \frac{1}{M}\sum_{j=1}^{M}\big|\widetilde{\phi}_{j,i}^{\mathrm{ref}}(t) - \phi_{j,i}^M(t)\big|, \quad i = 1, \ldots, N.$$

The total approximate L^1 error at time t is defined as $e_{\mathrm{tot}}(t) := e_1(t) + \cdots + e_N(t)$.

For Examples 3 to 6, we consider for overall tests, the physical parameters, densities $\varrho_{\mathrm{s}} = 2790\mathrm{kg/m^3}$, $\varrho_{\mathrm{f}} = 1280\mathrm{kg/m^3}$, $g = 9.81\mathrm{m/s^2}$, $\mu_{\mathrm{f}} = 0.02416\mathrm{Pa}$, and $D_1 = 1.25 \times 10^{-4}\mathrm{m}$. In (2.6) the hindered settling

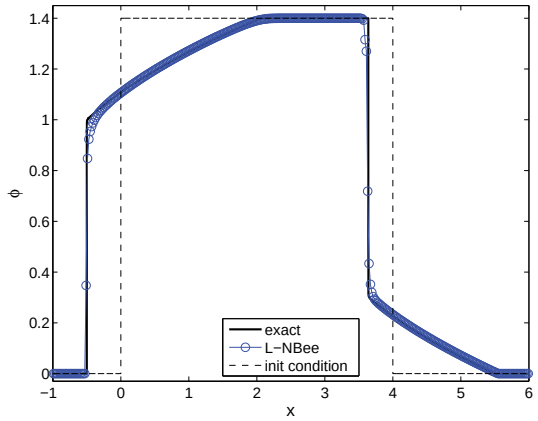

FIGURE 4. Example 1 ($N = 1$, $v(\phi)$ and $v'(\phi)$ with variable sign): numerical solution by L-NBee scheme at $T = 2$ with $\Delta x = 1/50$ compared with the exact entropy solution.

factor $V(\phi)$ is abruptly cut off at $\phi_{\max}$. However, to avoid spurious oscillations in the implementation of code we replace (2.6) by a Lipschitz continuous form of $V(\phi)$ defined by

$$V(\phi) = \begin{cases} (1-\phi)^{n_{\mathrm{RZ}}} & \text{if } 0 \le \phi \le \phi_{\mathrm{c}}, \\ (1-\phi_{\mathrm{c}})^{n_{\mathrm{RZ}}} \dfrac{\phi_{\max} - \phi}{\phi_{\max} - \phi_{\mathrm{c}}} & \text{if } \phi_{\mathrm{c}} \le \phi \le \phi_{\max}, \end{cases}$$

where ϕ_{c} is a number chosen in a way that $V'(\phi_{\mathrm{c}}) = V(\phi_{\mathrm{c}})/(\phi_{\mathrm{c}} - \phi_{\max})$. Analogous formulas replace $V_i(\phi)$ given by (2.7) and (2.11) for the MMLB and DG models, respectively.

4.1. **Example 1: $N = 1$, $v(\phi)$ and $v'(\phi)$ with variable sign.** In this test, we consider $v(\phi) = (1-\phi)^2 - 1/4$ for $0 \le \phi \le 3/2$. In this case $v(\phi)$ changes sign at $\phi = 1/2$ and $v'(\phi) \le 0$ for $0 < \phi < 1$ and $v'(\phi) > 0$ for $1 < \phi < 3/2$. The initial condition $\phi(x, 0) = 1.4\chi_{[0,4]}(x)$, for $-1 \le x \le 6$. In Figure 4 we plot the numerical solution obtained by the L-NBee scheme with the numerical flux (3.22) at $T = 2$ with $\Delta x = 1/50$ and compare the result with the exact entropy solution. We observe that the numerical solution approaches adequately entropy shocks and rarefaction waves, which corroborates the theoretical result of Theorem 3.4 that implies that the scheme converges to a weak solution.

4.2. **Example 2: $N = 1$, $v(\phi) \ge 0$ and $v'(\phi) \le 0$.** We consider the scalar equation (1.6) with the velocity function $v(\phi) = -0.01(1-\phi)^{4.65} < 0$ with $v'(\phi) > 0$ for all $0 \le \phi \le \phi_{\max} = 0.7$ and zero-flux boundary conditions. This scenario corresponds to the settling of an initially homogeneous, monodisperse suspension in a column of $L = 1$m with $\phi^0(x) = 0.35$ and $\phi_{\max} = 0.7$ [22]. In Figure 5 we display the numerical solution obtained with L-NBee scheme with $\Delta x = 1/200$ at two different times and compare results with the entropy solution. For this case, the entropy solution contains a shock and a rarefaction wave. We observe that L-NBee scheme adequately approximates the shock, but it is more diffusive when it approaches the rarefaction wave.

4.3. **Examples 3 and 4: $N = 2$ and $N = 11$, MLB model.** We utilize the MLB model described in Section 2.1.1. Example 3 corresponds to a standard test case of batch settling of an initially homogeneous suspension in a column of (unnormalized) height 0.3 m, corresponding to two ($N = 2$) species with normalized diameters $(d_1, d_2) = (1, 0.25202)$. Other parameters are $\phi_{\max} = 0.68$, $n_{\mathrm{RZ}} = 4.7$, and the initial concentrations are $\Phi^0 = (0.2, 0.05)$. These parameters correspond to experimental data by Schneider et al. [28]. For this test, $v_1(\Phi^0) > 0$ and $v_2(\Phi^0) < 0$. In Figure 6 (a) we display the numerical solution at time $T = 50$ obtained by the L-NBee scheme and $\Delta x = 1/6400$. In Figures 6 (c)–(f) we provide enlarged views of areas of interest of Figure 6 (a), and compare the numerical solutions with $\Delta x = 1/200$ for the

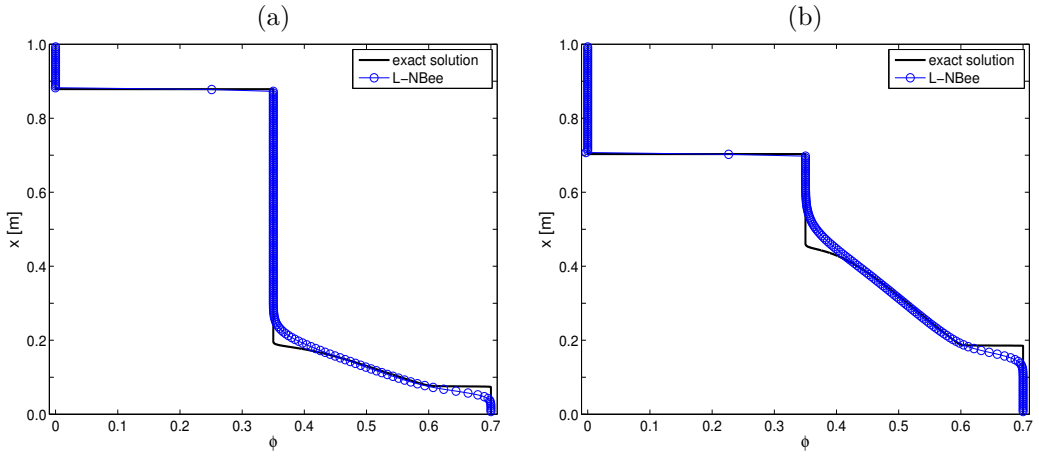

FIGURE 5. Example 2 ($N = 1$, $v(\phi) \geq 0$ and $v'(\phi) \leq 0$): numerical solution by L-NBee scheme with $\Delta x = 1/200$ at (a) $T = 90\,\mathrm{s}$, (b) $T = 220\,\mathrm{s}$ compared with the exact entropy solution.

i	1	2	3	4	5	6	7	8	9	10	11
$\phi_i^0[10^{-3}]$	0.435	3.747	14.420	32.603	47.912	47.762	32.663	15.104	4.511	0.783	0.060
$D_i[10^{-5}]$	8.769	8.345	7.921	7.497	7.073	6.649	6.225	5.801	5.377	4.953	4.529
d_i	1.000	0.952	0.903	0.855	0.807	0.758	0.710	0.662	0.613	0.565	0.516

TABLE 1. Example 4 ($N = 11$, MLB model): initial concentrations ϕ_i^0, real and normalized particles sizes D_i and d_i.

L-NBee and L-NBee-MUSCL schemes and Scheme 10 with the reference solution obtained by the WENO-SPEC-INT scheme. We observe that the L-NBee scheme adequately approximates the shocks, but is more diffusive when approaching rarefaction waves. The L-NBee-MUSCL scheme approximates adequately both shocks and rarefaction waves. In Figure 6 (b) we plot the approximate L^1-error versus the spatial discretization for all schemes, where we have included results of Scheme 8. It shows that for a given discretization, errors produced by the L-NBee scheme are smaller than those generated by Scheme 8, and errors by the L-NBee-MUSCL scheme are smaller than those of Scheme 10.

Example 4 corresponds to the settling of a suspension of $N = 11$ species in a column of (unnormalized) height $0.935\,\mathrm{m}$, the initial concentrations ϕ_i^0, diameters D_i, and normalized diameters $d_i = D_i/D_1$ given in Table 1, and the maximum total concentration $\phi_{\max} = 0.641$. The other parameters are the same as in Example 3. This example is based on a discrete approximation [30] for a suspension of closely sized spherical particles with continuously, roughly normally distributed particle sizes [29], see [14].

In Figure 7 (a) we display the numerical solution at time $T = 230$ obtained by the L-NBee scheme with $\Delta x = 1/6400$. In Figures 7 (d), (e) and (f) we provide enlarged views of areas interest for selected species. As in Example 3, we observe that the L-NBee scheme adequately approximates the shocks, but is more diffusive when it is approaching rarefaction waves, while the L-NBee-MUSCL scheme adequately approximates both shocks and rarefaction waves. In Figure 7 (b) we provide error histories and in Figure 7 (c) the corresponding efficiency (error reduction versus CPU time). We observe that error for L-NBee-MUSCL is smaller than for L-NBee, but in both cases errors are larger compared with those of WENO-SPEC-INT at the same discretization. However, according to Figure 7 (c) L-NBee schemes execute faster since these schemes do not need to compute spectral information of the flux Jacobian (as does WENO-SPEC-INT).

4.4. **Example 5 ($N = 4$, MMLB model).** We consider a polydisperse suspension with $N = 4$, with normalized particles sizes $(d_1, \ldots, d_4) = (1, 0.8, 0.6, 0.2)$, $(n_{\mathrm{RZ},1}, \ldots, n_{\mathrm{RZ},4}) = (3.8, 4.1, 4.4, 4.7)$, $\phi_{\max} = 0.68$,

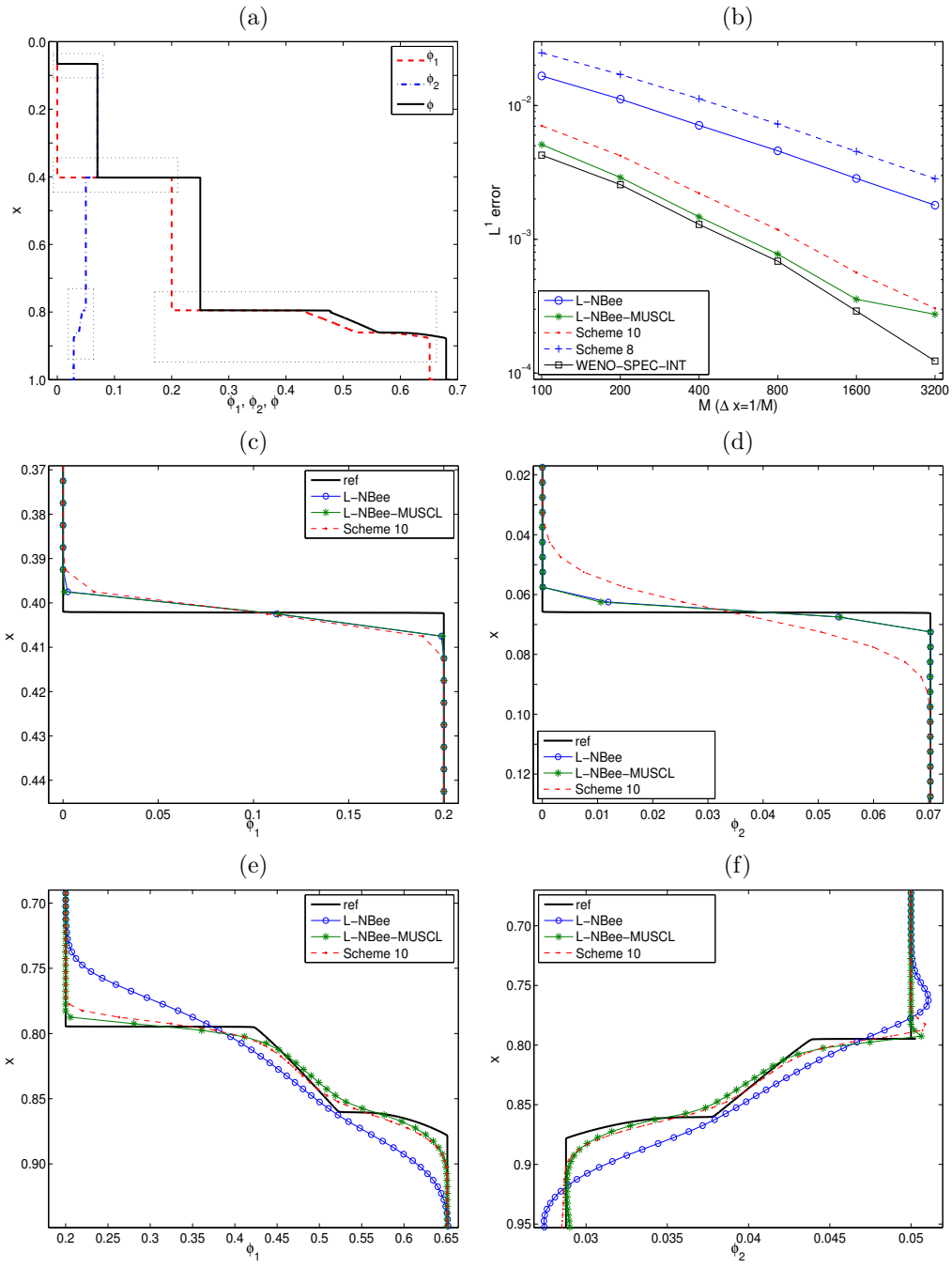

FIGURE 6. Example 3 ($N = 2$, MLB model: (a) numerical solution with L-NBee scheme at $T = 50$ with $\Delta x = 1/6400$, (b) approximate L^1-errors versus $M = 1/\Delta x$, (c, d, e, f) enlarged views of areas of interest and comparison of numerical solutions with $\Delta x = 1/200$.

and $\Phi^0 = (0.1, 0.1, 0.1, 0.1)$ for $0 \le x \le 1\,\mathrm{m}$. The other parameters are the same as in Example 3. For this example, $v_1(\Phi^0), v_2(\Phi^0)$ and $v_3(\Phi^0)$ are nonnegative, and $v_4(\Phi^0) < 0$. In Figure 8(a) we display the numerical solution obtained with L-NBee with $M = 3200$ cells at simulated time $T = 120$. Only for this

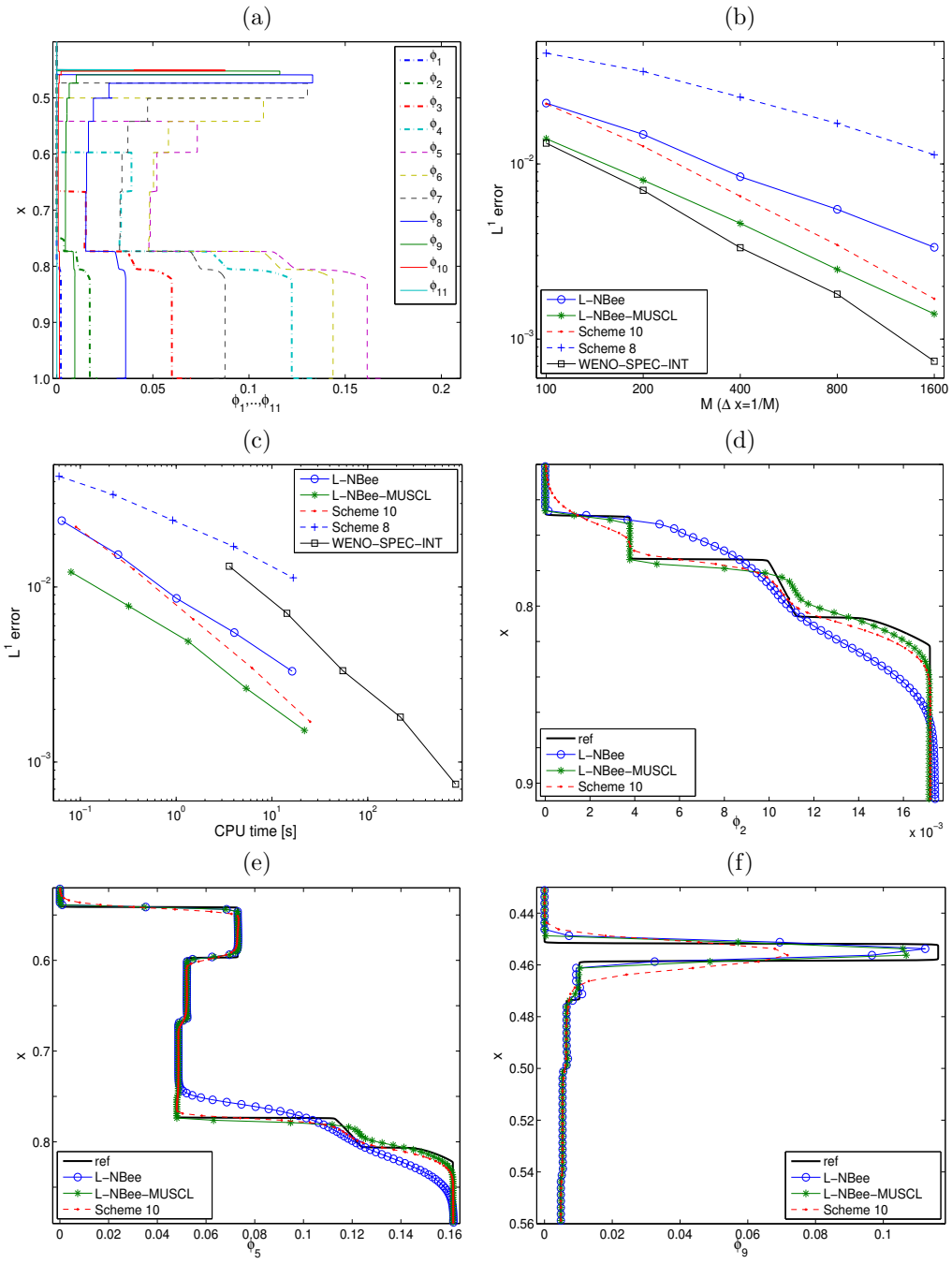

FIGURE 7. Example 4 ($N = 11$, MLB model): (a) numerical solution by L-NBee scheme at $T = 230$ with $\Delta x = 1/6400$, (b) approximate L^1-errors, (c) approximate L^1-errors versus CPU time, (d, e, f) enlarged views of interesting areas of (a) and comparison of numerical solutions with $\Delta x = 1/400$.

example, the reference solution is computed by the WENO-GHLL scheme introduced in [25] since it is easier to implement for this model than WENO-SPEC-INT. As in Examples 3 and 4, the L-NBee scheme does not

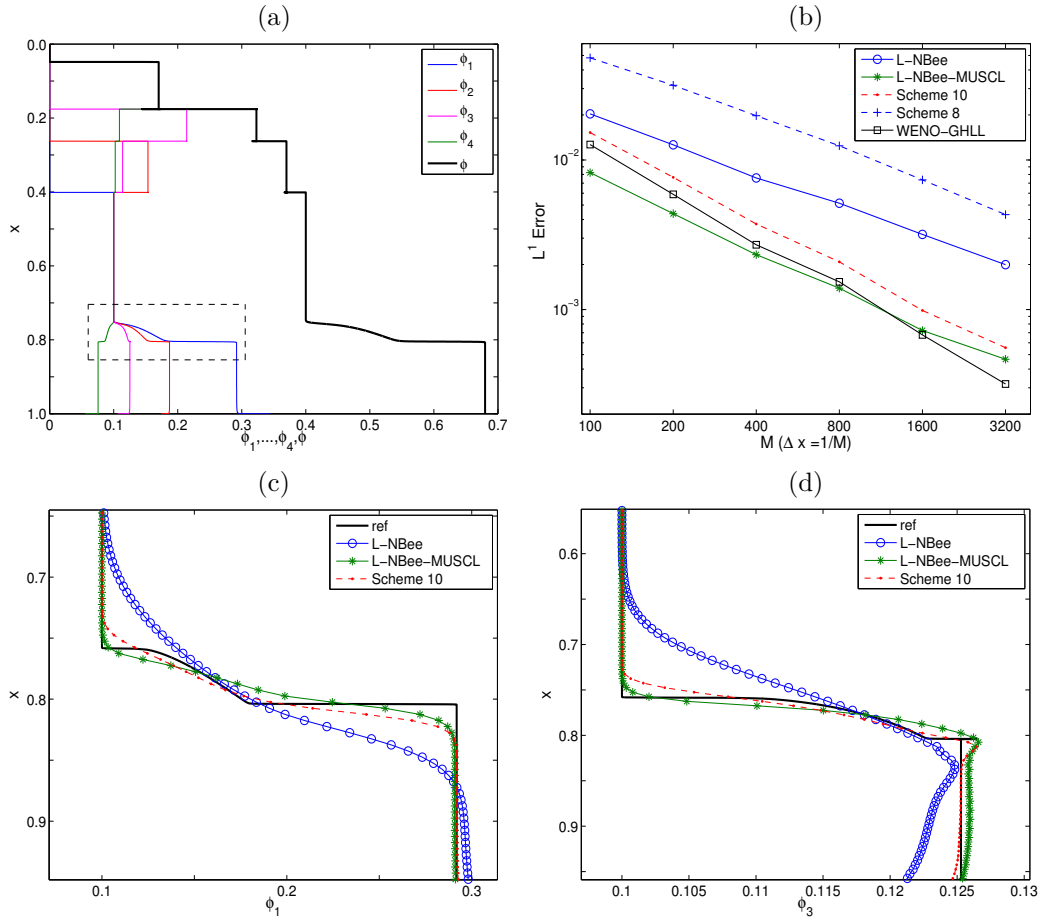

FIGURE 8. Example 5. MMLB model ($N = 4$, MMLB model): (a) numerical solution obtained at $T = 120$, (b) approximate L^1-errors versus $M = 1/\Delta x$ and (c, d) enlarged views of marked area in (a).

introduce numerical diffusion to approximate shock waves, but it is more diffusive for the approximation of rarefaction waves. On the other hand, L-NBee-MUSCL scheme adequately approaches shock and rarefaction waves.

We observe that the sedimentation process is adequately approximated by L-NBee schemes. Figures 8 (c) and (d) correspond to enlarged views of an area of Figure 8 (a) for selected species. We observe that the L-NBee scheme with MUSCL extrapolation gives the lowest errors for a given mesh with $M \leq 800$ and is thus even better than WENO-GHLL in these cases.

4.5. **Example 6 ($N = 4$, MLB, MMLB and DG models).** In this example, we compare the MLB, MMLB and DG models. We consider $N = 4$, $\Phi^0 = (0.1, 0.1, 0.1, 0.1)^{\mathrm{T}}$, $\phi_{\max} = 0.7$ and normalized squared sizes $\boldsymbol{\delta} = (1.0, 0.75, 0.50, 0.26)^{\mathrm{T}}$. Physical parameters are similar to Example 3. For the MLB model we consider $n_{\mathrm{RZ}} = 4.7$, for the MMLB model, $(n_{\mathrm{RZ},1}, \ldots, n_{\mathrm{RZ},4}) = (3.8, 4.1, 4.4, 4.7)$ and for the DG model, the parameter vector (2.10). In Figure 9, we display the numerical solution with L-NBee scheme with $\Delta x = 1/1600$ for each model at three simulated times.

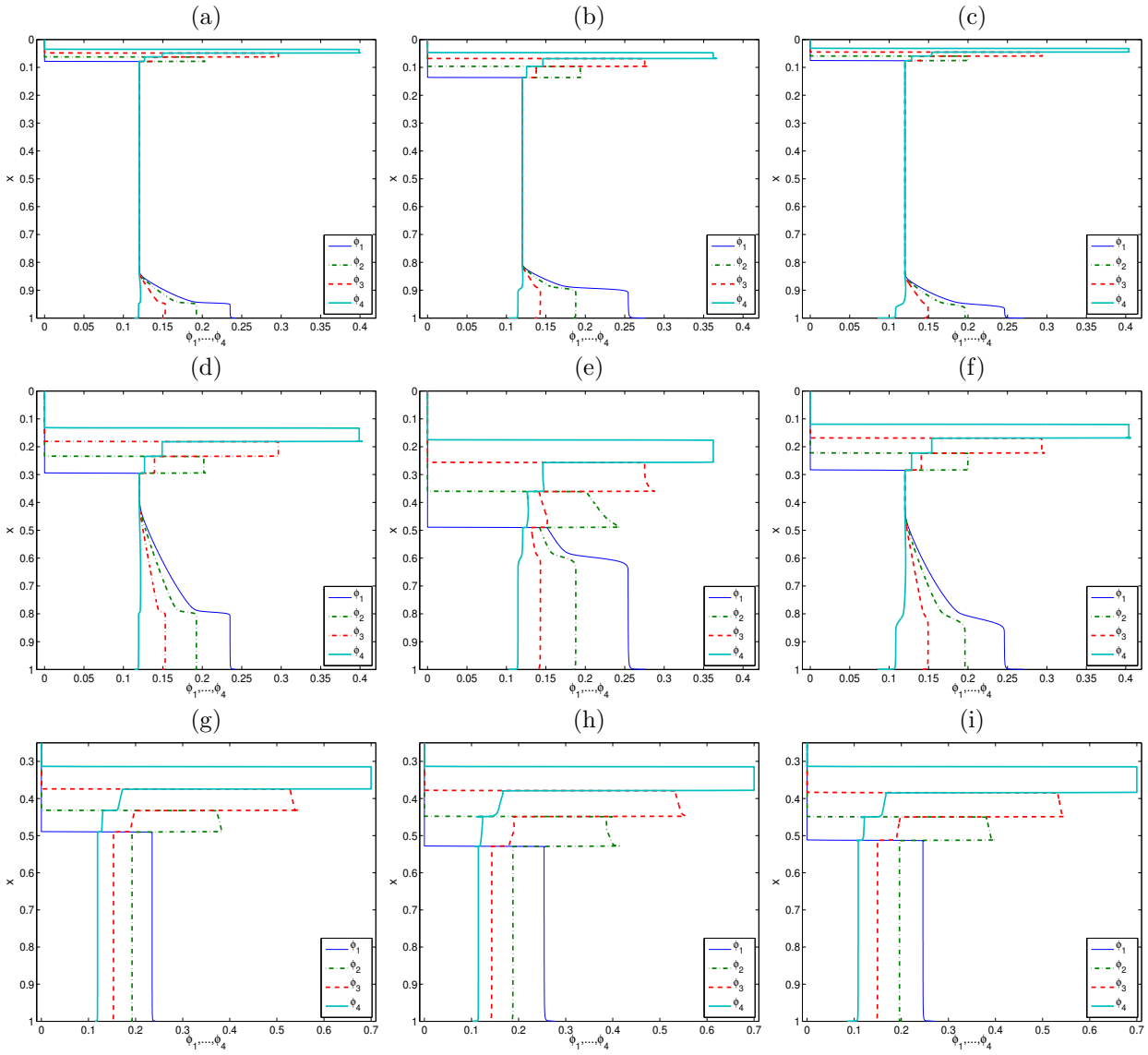

FIGURE 9. Example 6 ($N = 4$, MLB, MMLB and DG models): numerical solution by the L-NBee scheme with $\Delta x = 1/1600$ for (a, d, g) the DG model, (b, e, h) the MMLB model and (c, f, i) the MLB model at simulate times (a, b, c) $T = 50$, (d, e, f) $T = 300$ and (g, h, i) $T = 1500$.

5. Conclusions

We have extended the L-NBee schemes proposed in [8] to polydisperse models where velocities and their derivatives can change sign, and a partial numerical analysis has been provided in the scalar case. The proposed numerical scheme turns out to be competitive with existing scheme in the literature, which is especially interesting for large values of N (cf. Example 4). We observe in this case that the L-NBee-MUSCL scheme (the L-NBee scheme combined with MUSCL approach) provides the lowest (approximate) L^1 errors for a given CPU time, while it may not give the lowest L^1 errors for a given mesh size. In other words, of all schemes tested this scheme is most efficient in reduction of error. Finally, we mention that

the accuracy of the L-NBee-MUSCL scheme can be further enhanced by a full second-order discretization in both space and time. This will be considered in a forthcoming paper.

Acknowledgements

RB is supported by Fondecyt project 1130154; BASAL project CMM, Universidad de Chile and Centro de Investigación en Ingeniería Matemática (CI^{2}MA), Universidad de Concepción; Conicyt project Anillo ACT1118 (ANANUM); Red Doctoral REDOC.CTA, MINEDUC project UCO1202; and CRHIAM, project CONICYT/FONDAP/15130015. LMV is supported by Fondecyt project 11140708.

References

[1] J. Anderson, A secular equation for the eigenvalues of a diagonal matrix perturbation, Linear Algebra Appl. 246 (1996) 49–70.
[2] D.K. Basson, S. Berres, R. Bürger, On models of polydisperse sedimentation with particle-size-specific hindered-settling factors, Appl. Math. Modelling 33 (2009) 1815–1835.
[3] G.K. Batchelor, Sedimentation in a dilute polydisperse system of interacting spheres. Part 1. General theory, J. Fluid Mech. 119 (1982) 379–408.
[4] G.K. Batchelor, C.S. Wen, Sedimentation in a dilute polydisperse system of interacting spheres. Part 2. Numerical results, J. Fluid Mech. 124 (1982) 495–528.
[5] S. Benzoni-Gavage, R.M. Colombo, An n-populations model for traffic flow, Eur. J. Appl. Math. 14 (2003) 587–612.
[6] O. Bokanowski, H. Zidani, Anti-dissipative schemes for advection and application to Hamilton-Jacobi-Bellman equations, J. Sci. Comput. 30 (2007) 1–33.
[7] F. Bouchut, An antidiffusive entropy scheme for monotone scalar conservation laws, J. Sci. Comput. 21 (2004) 1–30.
[8] R. Bürger, C. Chalons, L.M. Villada, Antidiffusive and random-sampling Lagrangian-remap schemes for the multiclass Lighthill-Whitham-Richards traffic model, SIAM J. Sci. Comput. 35 (2013) B1341–B1368.
[9] R. Bürger, R. Donat, P. Mulet, C.A. Vega, Hyperbolicity analysis of polydisperse sedimentation models via a secular equation for the flux Jacobian, SIAM J. Appl. Math. 70 (2010) 2186–2213.
[10] R. Bürger, R. Donat, P. Mulet, C.A. Vega, On the implementation of WENO schemes for a class of polydisperse sedimentation models, J. Comput. Phys. 230 (2011) 2322–2344.
[11] R. Bürger, R. Donat, P. Mulet, C.A. Vega, On the hyperbolicity of certain models of polydisperse sedimentation, Math. Meth. Appl. Sci. 35 (2012) 723–744.
[12] R. Bürger, A. García, K.H. Karlsen, J.D. Towers, A family of numerical schemes for kinematic flows with discontinuous flux, J. Eng. Math. 60 (2008) 387–425.
[13] R. Bürger, K.H. Karlsen, E.M. Tory, W.L. Wendland, Model equations and instability regions for the sedimentation of polydisperse suspensions of spheres, ZAMM Z. Angew. Math. Mech. 82 (2002) 699–722.
[14] R. Bürger, A. Kozakevicius, Adaptive multiresolution WENO schemes for multi-species kinematic flow models, J. Comput. Phys. 224 (2007) 1190–1222.
[15] R.H. Davis, H. Gecol, Hindered settling function with no empirical parameters for polydisperse suspensions, AIChE J. 40 (1994) 570575.
[16] B. Després, F. Lagoutière, Contact discontinuity capturing schemes for linear advection and compressible gas dynamics, J. Sci. Comput. 16 (2001) 479–524.
[17] R. Donat, P. Mulet, Characteristic-based schemes for multi-class Lighthill-Whitham-Richards traffic models, J. Sci. Comput. 37 (2008) 233–250.
[18] R. Donat, P. Mulet, A secular equation for the Jacobian matrix of certain multi-species kinematic flow models, Numer. Meth. Partial Diff. Eqns. 26 (2010) 159–175.
[19] E. Godlewski, P.-A. Raviart, Numerical Approximation of Hyperbolic Systems of Conservation Laws. Springer Verlag, New York (1996)
[20] K. Höfler, S. Schwarzer, The structure of bidisperse suspensions al low Reynolds numbers. In A.M. Sändig, W. Schiehlen and W.L. Wendland (eds.), Multifield Problems: State of the Art, Springer Verlag, Berlin, 42–49, 2000.
[21] S. Jaouen, F. Lagoutière, Numerical transport of an arbitrary number of components, Comput. Meth. Appl. Mech. Engrg. 196 (2007) 3127–3140 (2007)
[22] G.J. Kynch, A theory of sedimentation, Trans. Faraday Soc. 48 (1952) 166–176.
[23] F. Lagoutière, Stability of reconstruction schemes for hyperbolic PDEs, Commun. Math. Sci. 6 (2008) 57–70.
[24] M.S. Lockett, K.S. Bassoon, Sedimentation of binary particle mixtures, Powder Technol. 24 (1979) 1–7.
[25] M.C. Martí, P. Mulet, Some techniques for improving the resolution of finite difference component-wise WENO schemes for polydisperse sedimentation models, Appl. Numer. Math. 78 (2014) 1–33.
[26] J.H. Masliyah, Hindered settling in a multiple-species particle system, Chem. Engrg. Sci. 34 (1979) 1166–1168.
[27] J.F. Richardson, W.N. Zaki, Sedimentation and fluidization: Part I, Trans. Inst. Chem. Eng. (London) 32 (1954) 35–53.
[28] W. Schneider, G. Anestis, U. Schaflinger, Sediment composition due to settling of particles of different sizes, Int. J. Multiphase Flow 11 (1985) 419–423.

[29] P.T. Shannon, E. Stroupe, E.M. Tory, Batch and continuous thickening, Ind. Eng. Chem. Fund. 2 (1963) 203–211.
[30] E.M. Tory, R.A. Ford, M. Bargieł, Simulation of the sedimentation of monodisperse and polydisperse suspensions, in: W.L. Wendland, M. Efendiev (Eds.), Analysis and Simulation of Multifield Problems, Springer-Verlag, Berlin, 2003, pp. 343–348.
[31] B. van Leer, Towards the ultimate conservative difference scheme II. Monotonicity and conservation combined in a second order scheme, J. Comput. Phys. 14 (1974) 361–370.
[32] B. van Leer, Towards the ultimate conservative difference scheme. V. A second-order sequel to Godunov's method, J. Comput. Phys. 32 (1979) 101–136.
[33] B. van Leer, On the relation between the upwind-differencing schemes of Godunov, Engquist-Osher and Roe. SIAM J. Sci. Statist. Comput. 5 (1984) 1–20.
[34] G.C.K. Wong, S.C. Wong, A multi-class traffic flow model—an extension of LWR model with heterogeneous drivers, Transp. Res. A 36 (2002) 827–841.

Centro de Investigación en Ingeniería Matemática (CI^{2}MA)

PRE-PUBLICACIONES 2014 - 2015

2014-28 Fabián Flores-Bazán, Giandomenico Mastroeni: *Characterizing FJ and KKT conditions in nonconvex mathematical programming with applications*

2014-29 Franco Fagnola, Carlos M. Mora: *On the relationship between a quantum Markov semigroup and its representation via linear stochastic Schrodinger equations*

2014-30 Julio Aracena, Luis Gomez, Lilian Salinas: *Complexity of limit cycle existence and feasibility problems in Boolean networks*

2014-31 Raimund Bürger, Stefan Diehl, Thomas Maere, Ingmar Nopens, Elena Torfs: *Impact on sludge inventory and control strategies using the Benchmark Simulation Model No. 1 with the Bürger-Diehl settler model*

2014-32 Gabriel N. Gatica, Luis F. Gatica, Filander A. Sequeira: *Analysis of an augmented pseudostress-based mixed formulation for a nonlinear Brinkman model of porous media flow*

2014-33 Jessika Camaño, Ricardo Oyarzúa, Giordano Tierra: *Analysis of an augmented mixed-FEM for the Navier-Stokes problem*

2014-34 Mario Álvarez, Gabriel N. Gatica, Ricardo Ruiz-Baier: *Analysis of a vorticity-based fully-mixed formulation for the 3D Brinkman-Darcy problem*

2014-35 Julien Deschamps, Erwan Hingant, Romain Yvinec: *From a stochastic Becker-Doring model to the Lifschitz-Slyozov equation with boundary value*

2015-01 Sebastian Dominguez, Gabriel N. Gatica, Antonio Marquez, Salim Meddahi: *A primal-mixed formulation for the strong coupling of quasi-Newtonian fluids with porous media*

2015-02 Felipe Lepe, David Mora, Rodolfo Rodríguez: *Finite element analysis of a bending moment formulation for the vibration problem of a non-homogeneous Timoshenko beam*

2015-03 Fabián Flores-Bazán, Fernando Flores-Bazán, Cristian Vera: *Maximizing and minimizing quasiconvex functions: related properties, existence and optimality conditions via radial epiderivatives*

2015-04 Raimund Bürger, Christophe Chalons, Luis M. Villada: *Antidiffusive Lagrangian-remap schemes for models of polydisperse sedimentation*

Para obtener copias de las Pre-Publicaciones, escribir o llamar a: Director, Centro de Investigación en Ingeniería Matemática, Universidad de Concepción, Casilla 160-C, Concepción, Chile, Tel.: 41-2661324, o bien, visitar la página web del centro: `http://www.ci2ma.udec.cl`







Centro de Investigación en
Ingeniería Matemática (CI²MA)
Universidad de Concepción

Casilla 160-C, Concepción, Chile
Tel.: 56-41-2661324/2661554/2661316
http://www.ci2ma.udec.cl